eLife

Reviewed Preprint
v2 • December 16, 2024
Revised by authors

Reviewed Preprint
v1 • September 12, 2024

Neuroscience

Aberrant FGF signaling promotes granule neuron precursor expansion in SHH subgroup infantile medulloblastoma

Odessa R Yabut, Hector Gomez, Jessica Arela, Jesse Garcia Castillo, Thomas Ngo, Samuel J Pleasure

Department of Neurology, Weill Institute for Neuroscience, University of California San Francisco, San Francisco, United States • Department of Psychiatry, Weill Institute for Neuroscience, University of California San Francisco, San Francisco, United States • Programs in Neuroscience and Developmental Biology, Eli and Edythe Broad Center of Regeneration Medicine and Stem Cell Research, University of California San Francisco, San Francisco, United States

eLife Assessment

This study provides **valuable** new insight into the role of Fgf signalling in SUFU mutation-linked cerebellar tumors and indicates novel therapeutic interventions via inhibition of Fgf signalling. The potential impact of this work is therefore very high and it is supported by **solid** evidence. However, due to current limitations in the full identification of the cell types secreting FGF5, and issues with robustness of evaluation of genetically engineered animals, the validation of some interpretations awaits future experiments.

https://doi.org/10.7554/eLife.100767.2.sa4

Abstract

Mutations in Sonic Hedgehog (SHH) signaling pathway genes, e.g., *Suppressor of Fused* (SUFU), drive granule neuron precursors (GNP) to form medulloblastomas (MB^{SHH}). However, how different molecular lesions in the Shh pathway drive transformation is frequently unclear, and *SUFU* mutations in the cerebellum seem distinct. In this study, we show that fibroblast growth factor 5 (FGF5) signaling is integral for many infantile MB^{SHH} cases and that *FGF5* expression is uniquely upregulated in infantile MB^{SHH} tumors. Similarly, mice lacking SUFU (Sufu-cKO) ectopically express *Fgf5* specifically along the secondary fissure where GNPs harbor preneoplastic lesions and show that FGFR signaling is also ectopically activated in this region. Treatment with an FGFR antagonist rescues the severe GNP hyperplasia and restores cerebellar architecture. Thus, direct inhibition of FGF signaling may be a promising and novel therapeutic candidate for infantile MB^{SHH}.

Introduction

Medulloblastoma (MB) is the most common malignant brain tumor in children, with half of cases diagnosed before the age of 5 (Ward et al., 2014; Ostrom et al., 2016). Mutations in *Suppressor of Fused* (*SUFU)* comprise approximately 30% of tumors in infants with Sonic Hedgehog-driven MB (MB^{SHH}). Infantile MB^{SHH}, including those associated with *SUFU* mutations ($MB^{SHH\text{-}SUFU}$), has a worse prognosis and higher rates of local recurrence than other MB^{SHH} subtypes (Kool et al., 2014; Schwalbe et al., 2017; Guerrini-Rousseau et al., 2018). Unfortunately, available SHH-targeted treatments for MB^{SHH} act specifically on proteins upstream of SUFU, and are therefore ineffective for $MB^{SHH\text{-}SUFU}$ patients (Kool et al., 2014). The poor prognosis, early occurrence, and lack of targeted therapy for $MB^{SHH\text{-}SUFU}$ patients make a detailed understanding of the drivers of oncogenesis in this group of great importance.

SUFU acts as an intracellular modulator of SHH signaling (Matise and Wang, 2011). Briefly, the SHH signaling pathway is initiated after the binding of extracellular Shh ligands to the transmembrane receptor Patched 1 (PTCH1). This relieves PTCH1 inhibition of the transmembrane protein, Smoothened (SMO), and enables the initiation of a cascade of intracellular events promoting the activator function of the transcription factors, GLI1, GLI2, or GLI3. SUFU modulates SHH signaling by ensuring the stability of GLI transcription factors or by promoting the formation of the repressor forms of GLI2 (GLI2R) or GLI3 (GLI3R) (Chen et al., 2009; Wang et al., 2010; Lin et al., 2014). Thus, depending on the developmental context, loss of SUFU can lead to activation or repression of SHH signaling. In the developing cerebellum, SUFU dysfunction is associated with the abnormal development of granule neuron precursors (GNP), which account for MB^{SHH} (Kim et al., 2011, 2018; Vanner et al., 2014; Kong et al., 2019; Vladoiu et al., 2019; Yin et al., 2019; Jiwani et al., 2020). GNPs populate the external granule layer (EGL) along the cerebellar perimeter, where local SHH signals trigger GNP proliferation and differentiation at neonatal stages. However, other mitogenic pathways can also influence GNP behavior (Leto et al., 2016), yet little is known about how SUFU interacts with these pathways. Understanding how *Sufu* loss-of-function (LOF) affects the activity of concurrent local signaling pathways in granule neuron development may be key to developing potent targets for anti-tumor therapy.

In this study, we examined the regulation of FGF signaling in MB^{SHH} and identified upregulation of *FGF5* expression in tumors of infantile MB^{SHH} patients. Similarly, we show ectopic expression of *Fgf5* in the neonatal cerebellum of mice lacking SUFU, which correlates with the activation of FGF signaling in surrounding EGL-localized cells where GNPs accumulate. Strikingly, acute pharmacological inhibition of FGF signaling results in near-complete rescue of these defects, including restoration of cerebellar histo-organization. Thus, our findings identify *FGF5* as a potential biomarker for a subset of patients with infantile MB^{SHH} who may be responsive to FGFR-targeting therapies.

Results

FGF5 is specifically upregulated in SHH-driven infantile MB

We previously reported that *Sufu* LOF in neocortical progenitors results in FGF signaling activation to influence the specification and differentiation of neocortical excitatory neurons (Yabut et al., 2020). Thus, we sought to determine if key FGF signaling pathway genes are differentially expressed in MB patient tumors. We performed a comparative analysis of the expression dataset from 763 MB patient samples comprised of tumors resected from molecularly distinct MB

subgroups: Wingless (Wnt subgroup; MB^{WNT}), MB^{SHH}, Group 3 (MB^{Group3}), and Group 4 (MB^{Group4}) (Cavalli et al., 2017). Strikingly, our analyses show that *FGF5* expression is higher in tumors, specifically from MB^{SHH} patients, compared to other MB subgroups, with approximately 25% of MB^{SHH} tumors exhibiting a two-fold increase (**Fig. 1A-1B**). We also find that *FGF5* is uniquely upregulated in MB^{SHH} tumors from patients within the 0-3 years old age group, but not patients within the same age group in other MB subtypes (**Fig. 1C**). Further examination across all MB^{SHH} tumors stratified which subgroups express the highest levels of *FGF5* expression. Infantile tumors, largely belonging to the SHHb and SHHg subgroups (Cavalli et al., 2017), exhibit higher *FGF5* levels compared to tumors from children (SHHa) or adults (SHHd) (**Fig. 1D**). By all measures, the proportion of SHHb and SHHg tumors with relatively high levels of *FGF5* is significantly increased (~30%) compared to other MB^{SHH} subgroups (**Fig. 1E**). Taken together, these findings strongly suggest that FGF signaling is specifically disrupted in infantile-onset MB^{SHH}.

Region-specific expansion of GNPs in the P0 Sufu-cKO cerebellum coincides with increased *Fgf5* expression

FGF signaling has been implicated in cerebellar development (Yaguchi et al., 2009; Yu et al., 2011), leading us to wonder if and how aberrant FGF signaling may be contributing to the oncogenicity of GNPs. Since mutations in *SUFU* drive infantile MB^{SHH}, we generated the mutant mice (*hGFAP-Cre;Sufu*$^{fl/fl}$, hereto referred to as Sufu-cKO), in which *Sufu* is conditionally deleted in GNPs (Zhuo et al., 2001) to examine FGF activity. Sufu-cKO mice exhibit profound defects in cerebellar development. At P0, a time point at which GNP proliferation and differentiation is ongoing, there is a visible increase in measured cerebellar size and expansion of Pax6-positive (Pax6+) GNPs in the EGL of Sufu-cKO cerebellum compared to controls (**Fig. 2A-C**). Notably, the expansion of Pax6+ GNPs specifically localizes along the secondary fissure (EGL Region B, arrow in **Fig. 2A**) compared to other EGL areas (EGL Regions A and C) in the P0 Sufu-cKO cerebellum (**Fig. 2D**). We then proceeded to examine whether these defects correlated with abnormal FGF5 expression. We collected P0 littermates for these analyses and found that the foliation defects are particularly severe in the cerebelli of mice from this P0 Sufu-cKO litter compared to littermate controls (as determined by DAPI labeling in **Fig. 2E**). *In situ* hybridization (ISH) using *Fgf5*-specific riboprobes show high expression of *Fgf5* ($Fgf5^{high}$) immediately adjacent to the presumptive secondary fissure in the P0 control cerebellum (**Fig. 2E**). Strikingly, in the P0 Sufu-cKO cerebellum, there is an expansion of $Fgf5^{high}$ expression regions (**Fig. 2E**), coinciding with areas near the secondary fissure where GNP expansion is most severe (**Fig. 2A, 2D**). Further, while *Fgf5*-expressing (FGF5+) cells are largely excluded from the EGL of the control cerebellum, a substantial number of *Fgf5*+ cells are ectopically localized in the EGL Region B of the Sufu-cKO cerebellum (**Fig. 2E, 2F**). *Fgf5* mRNA molecules are visibly higher in *Fgf5*-expressing cells in the Sufu-cKO EGL, while *Fgf5* expression is largely absent in the deeper EGL regions (outlined cells within boxed regions in **Fig. 2F**). These findings implicate FGF5 as a potential instigator of region-specific defects in GNP differentiation present in the P0 Sufu-cKO cerebellum.

FGF signaling drives GNP proliferation in the P0 Sufu-cKO cerebellum

FGF5 is a ligand for fibroblast growth factor receptors 1 (FGFR1) and 2 (FGFR2), both of which are expressed in the developing cerebellum, particularly in IGL regions where *Fgf5*-expressing cells localize (Clements et al., 1993; Ornitz et al., 1996). The binding of FGF5 to these receptors triggers the activation of multiple intracellular signaling pathways, including the mitogen-activated protein kinase (MAPK) pathway, to control cellular activities driving NSC progression (**Fig. 3A**) (Ornitz and Itoh, 2015). Immunostaining with antibodies to detect MAPK pathway activation reveals increased MAPK activity in the EGL of the P0 Sufu-cKO cerebellum. Regional

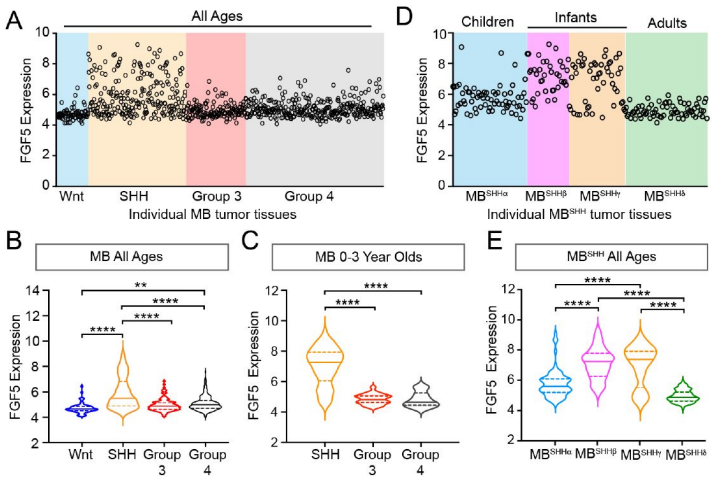

Figure 1

Upregulated *FGF5* expression in MB^{SHH} tumors from infant patients.

(A) Levels of FGF5 expression in human MB tumors of all ages from GEO expression dataset #GSE85217(Cavalli et al., 2017). **(B, C)** Statistical analysis of *FGF5* expression levels associated with MB tumor subtypes from patients across all ages (B) and 0-3 year old MB patients (C). **p<0.01, ****p<0.0001. **(D, E)** Graph represents *FGF5* expression levels in human MB^{SHH} tumors of all ages from GEO expression dataset #GSE85217 (D) and corresponding plots (E) showing statistically higher *FGF5* expression in tumors from infants with MB^{SHH} compared to tumors from children or adults with MB^{SHH}. ****p<0.0001.

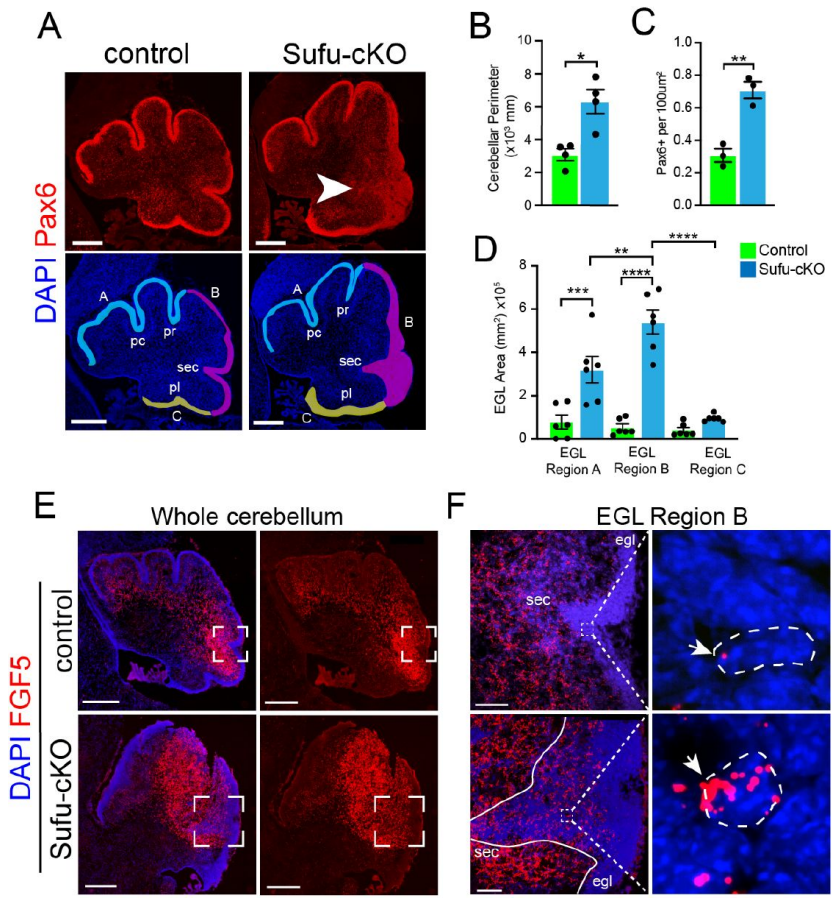

Figure 2

Increased FGF5 expression coincides with region-specific expansion of GNPs in the P0 Sufu-cKO cerebellum.

(A) Pax6 (red) and DAPI (blue) immunofluorescence staining of the P0 Sufu-cKO and control cerebelli. Arrow points to severely expanded EGL region B in the P0 Sufu-cKO cerebellum. EGL regions are designated in DAPI-labeled sections as A (light blue), B (magenta), and C (yellow). Each region encompasses specific fissures: the preculminate (pc) and primary (pr) fissures for Region A, the secondary (sec) fissure for Region B, and the posterolateral (pl) fissure for Region Scale bars: Scale bars = 250 mm. **(B-D)** Quantification and comparison of the cerebellar perimeter (B), total area occupied by densely packed Pax6+ cells (C), and size of specific EGL regions (D) between P0 Sufu-cKO and control cerebelli. **(E)** Fluorescent *in situ* hybridization using RNAScope probes against *Fgf5* mRNA (red) shows the expansion of *Fgf5* expression in the P0 Sufu-cKO cerebellum compared to controls. Sections are counterstained with DAPI to distinguish structures. Boxed areas are magnified in F. Scale bars = 500 mm. **(F)** *Fgf5* is ectopically expressed in cells within the EGL of the P0 Sufu-cKO cerebellum. Boxed areas within the EGL show DAPI-labeled cells expressing visibly high levels of *Fgf5*, identified as punctate labeling (arrowheads), in the EGL of P0 Sufu-cKO cerebellum compared to controls. Scale bars = 50 mm. **p<0.05, **p<0.01, ***p<0.001, ****p<0.0001.

distribution of cells labeled with phospho-Erk1/2 (pErk1/2+), a marker for activated MAPK signaling, shows that the abnormally expanded EGL of the secondary fissure in the P0 Sufu-cKO cerebellum increase in these cells (**Fig. 3B**). We quantified the number of pERK1/2+ cells in proliferative regions defined by dense Ki-67-labeled cells and found a significant increase in pERK1/2+ cells compared to controls (**Fig. 3C**). Many pERK1/2+ cells are also proliferative as indicated by Ki-67 labeling (boxed areas, **Fig. 3B**) and the numbers of these dual labeled cells were significantly higher in the Sufu-cKO cerebellum compared to controls (**Fig. 3D**). These findings indicate that the increase in *Fgf5* expression correlates with the activation of FGF signaling in GNPs and demonstrates a likely role in regulating the abnormal proliferation and pre-neoplastic lesion in mutant mice.

Given the role of SUFU in regulating GLI transcription factors to modulate SHH signaling activity (Kim et al., 2018; Yin et al., 2019), we examined whether the activation of FGF signaling occurred [C.] concurrently with SHH signaling activation. Surprisingly, GLI protein levels in the P0 control and Sufu-cKO cerebellum show a marked reduction of GLI1, GLI2, GLI3, and PTCH1 levels (**Supplementary Fig. 1A**); this is inconsistent with elevated SHH signaling we anticipated in the absence of SUFU. To directly examine this in specific EGL regions, we compared the cerebellum of P0 control and Sufu-cKO mice carrying the Shh reporter transgene *Gli1-LacZ* (Bai et al., 2002). In these mice, Shh signaling activity is absent or very low throughout the entire P0 Sufu-cKO cerebellum but is highly active in a region-specific manner in controls (**Supplementary Fig. 1B**). Furthermore, while some LacZ+ cells are detectable in EGL regions A and C and adjacent ML and IGL, LacZ+ cells are completely absent in EGL region B and adjacent areas of the P0 Sufu-cKO cerebellum (**Supplementary Fig. 1B-1C**). These findings indicate that the accumulation of GNPs does not rely on active Shh signaling, particularly in Region B, where there is a severe expansion of GNPs in the absence of SUFU.

Blockade of FGF signaling dramatically rescues the Sufu-cKO phenotype

To determine if activated FGF signaling drives GNP defects in the Sufu-cKO cerebellum, we pharmacologically inhibited FGF signaling using the competitive FGFR1-3 antagonist AZD4547 (Gudernova et al., 2016). For this experiment, 1 µl of AZD4547 (5mg/ml) was delivered via intraventricular (IV) injection for 5 consecutive days beginning at P0, and the cerebellum was analyzed 3 days after treatment at P7 (**Fig. 3E**). Strikingly, AZD4547 treatment results in near complete rescue of the GNP phenotype by P7 in the Sufu-cKO cerebellum, displaying a cerebellar morphology indistinguishable from controls with normal foliation and cellular organization (**Fig. 3F**). Indeed, in the cerebellum of AZD4547 -treated P7 Sufu-cKO mice, proliferating Ki-67+ cells largely exclusively localize in the EGL while NeuN+ cells densely pack the IGL and not the EGL (**Fig. 3G**). Notably, NeuN expression appears in cells localized at the border of the EGL and ML, where Ki-67+ cells are absent, indicating that post-mitotic cells successfully began differentiation as observed in controls (boxed regions, **Fig. 3G**). Thus, our findings confirm that inhibition of FGF signaling in proliferating GNPs of the Sufu-cKO cerebellum ensure normal progression of GNP differentiation.

Fgf5 expression is increased in the developing cerebellum of Sufu;p53-dKO mice

Our findings indicate a critical role for FGF signaling in driving GNP hyperplasia, making GNPs vulnerable to neoplastic lesions, resulting in tumorigenesis when SUFU is absent in the developing cerebellum. Indeed, we find that Pax6+ GNPs within the neonatal Sufu-cKO EGL display an increase in double-strand breaks, especially in Region B (DSBs; **Fig. 4A-4B**), as detected by immunostaining for phosphorylated H2AX (γH2AX), an early marker for DSBs (Mah et al., 2010). Nevertheless, as previously reported, tumors do not readily form in the Sufu-cKO cerebellum (Yin et al., 2019), indicating either timely repair of DSBs or the induction of apoptosis in GNPs with

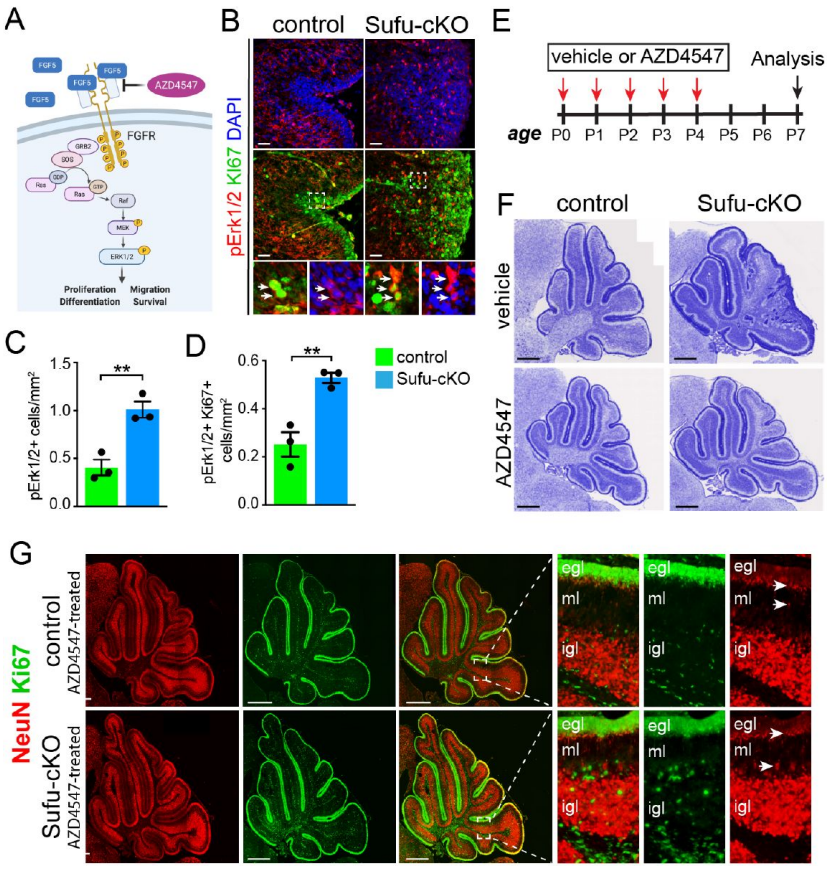

Figure 3

Ectopic activation of FGF signaling in the EGL of P0 Sufu-cKO cerebellum.

(A) Schematic diagram showing the activation of FGF signaling activity upon binding of FGF5 to extracellular domains of FGFR via the MAPK signal transduction pathway. **(B)** Double-immunofluorescence staining with Ki-67 (green) and phospho-Erk1/2 (pErk1/2; red), a marker of activated MAPK signaling in the P0 Sufu-cKO and control cerebelli. Boxed regions show pErk1/2+ and Ki-67+ cells (arrowheads) in the control and Sufu-cKO EGL. Scale bars = 50 μm. **(C, D)** Quantification of pErk1/2+ cells (C) and double-labeled pErk1/2+ and Ki-67+ cells (D) in the P0 Sufu-cKO and control EGL Region B. **p<0.01. **(E)** Experimental design of rescue studies performed by intraventricular administration of FGFR1-3 pharmacological inhibitor, AZD4547, or vehicle controls. **(F)** Nissl staining of the P7 control and Sufu-cKO treated with either AZD4547 or vehicle, 2 days after treatment. Scale bars = 500 μm. **(G)** NeuN and Ki-67 double immunofluorescence staining of the P7 control and Sufu-cKO treated with AZD4547. Boxed regions show localization and organization of NeuN+ and Ki-67+ cells in distinct cerebellar layers. Arrows point to areas of the EGL and IGL where NeuN+ cells are beginning to be expressed.
Created with *BioRender.com/g44j117*.

significant genomic instability. Indeed, double-labeling with cleaved Caspase 3 (CC3) and γH2AX shows a significantly higher number of double-labeled cells in EGL Regions A and B (**Supplementary Fig. 2A-2B**). Among the downstream targets of DSB repair pathways is p53, which, when activated, mediates cell death to suppress tumor formation (Gao et al., 2000). In the P0 Sufu-cKO cerebellum, p53 protein is present, albeit significantly reduced (**Fig. 4C**). The reduction in p53 may be driving an increase in DSBs, yet it is still sufficient to induce apoptotic pathways. Supporting this, conditional ablation of both *p53* and *Sufu* in GNPs (*hGFAP-Cre;Sufu*$^{fl/fl}$;*p53*$^{fl/fl}$ or Sufu;p53-dKO) results in the formation of massive tumors in the cerebellum within 2 months after birth (**Fig. 4F**), indicating the failure to activate critical apoptotic pathways. However, tumors do not form in mice lacking *p53* (Marino et al., 2000) or *Sufu* alone (**Fig. 4F**). These findings suggest that in the absence of SUFU, the failure of GNPs to transition into fully differentiated granule neurons compromises genomic stability and renders GNPs extremely vulnerable to tumor formation with a second molecular hit.

We sought to confirm that upregulated FGF signaling also occurs in the tumor-prone Sufu;p53-dKO. As expected, the neonatal cerebellum of Sufu-cKO displays EGL expansion due to excess proliferative (Ki-67+) and Pax6+ cells in the P0 Sufu;p53-dKO cerebellum but not in p53-cKO and control cerebelli (**Fig. 4G**). Further expansion of Pax6+ GNPs in the P0 Sufu;p53-dKO is also most severe along the secondary fissure (EGL Region B) compared to other EGL areas (EGL Regions A and C) of the P0 Sufu;p53-dkO cerebellum (**Fig. 4G-4H**). As with our observations in the P0 Sufu-cKO cerebellum, ISH for *Fgf5* in the P0 Sufu;p53-dKO cerebellum shows ectopic *Fgf5* expression. Particularly, *Fgf5*+ cells are expanded anteriorly and detected specifically around the secondary fissure of the P0 Sufu;p53-dKO cerebellum (**Fig. 4I**). There is also ectopic MAPK signaling activity in the P0 Sufu;p53-dKO cerebellum, with significantly higher numbers of pErk1/2+ cells within the EGL, many of which are proliferative as marked by co-labeling with Ki-67, within the expanded EGL of the secondary fissure (**Fig. 4J**). These findings indicate that, as in the P0 Sufu-cKO cerebellum, ectopic *Fgf5* expression triggers FGF signaling in GNPs in the P0 Sufu;p53-dKO cerebellum and may facilitate oncogenic transformation and tumor growth of GNPs.

Discussion

Our studies identify a mechanism by which the combinatorial effects of oncogenic *SUFU* mutations and other concurrent developmental signaling pathways make GNPs vulnerable to oncogenic transformation leading to infantile MB^{SHH}. Using mice lacking *Sufu* in GNPs, we find that ectopic *Fgf5* expression correlates with an increase in FGF signaling, particularly in areas where proliferating GNPs reside, resulting in GNP hyperplasia, preneoplastic lesions, and patterning defects. Inhibition of Fgf signaling through pharmacological blockade of FGFR1-3 prevents hyperplasia and associated cerebellar architectural abnormalities. Strongly supporting a role for FGF5, we also find elevated levels of *Fgf5* gene expression specifically in infantile MB^{SHH} patients, but not in other MB subgroups. These findings indicate that FGF-targeting compounds may be a promising therapeutic option for infantile MB^{SHH} patients, with elevated levels of FGF5 in tumor tissues acting as a potential biomarker.

Expansion of Pax6+ GNPs in the newborn Sufu-cKO cerebellum (**Fig. 2**) occurs in the posterior/ventral regions of the cerebellar hemispheres where infantile MB tumors typically arise (Tan et al., 2018). Interestingly, these subregions have low levels of GLI1 reporter activity, PTCH1 expression, and SHH ligand expression (Corrales et al., 2004). Spatially distinct regulation of granule neuron development by SUFU may, therefore, rely on non-canonical SHH signaling beyond SMO or through yet undefined downstream interactions, resulting in control of FGF signaling activity. Supporting this, we find ectopic expression of *Fgf5* and deregulation of FGF signaling as marked by the excessive intracellular activation of MAPK signaling in the P0 Sufu-cKO cerebellum. Similarly, in previous studies, ectopic expression of FGF ligands, *Fgf8* and *Fgf15*, are associated with degradation of GLI3R because of *Sufu* deletion, resulting in regional patterning

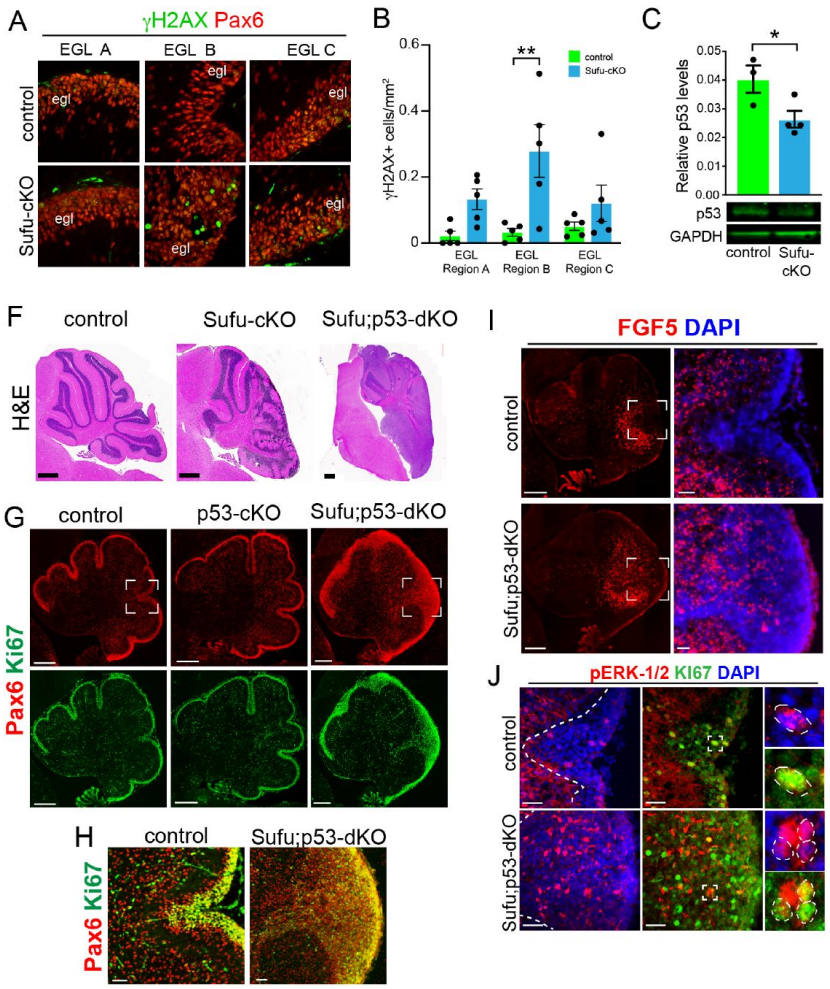

Figure 4

Evidence of pre-neoplastic lesions and high rates of cell death in Sufu-cKO granule neuron precursors.

(A) Double-immunofluorescence staining with Pax6 (red) and (γH2AX (green), a marker for double-strand DNA breaks in specific EGL regions of the P0 Sufu-cKO and control cerebella. **(B)** Quantification of (γH2AX + cells in each cerebellar region of P0 control and Sufu-cKO mice. **p<0.01. **(C)** Western blot analysis of p53 protein levels in P0 control and Sufu-cKO cerebellar protein lysates. *p<0.05. **(F)** Hematoxylin and Eosin (H&E) staining of P60 control, Sufu-cKO, Sufu;p53-dKO cerebella. Scale bars = 500 μm. **(G, H)** Double-immunofluorescence staining against Pax6 (red) and Ki-67 (green) in the P0 control, p53-cKO, and Sufu;p53-dKO cerebellum (G). Boxed regions in G are magnified in H, demonstrating the expansion of the EGL in the P0 Sufu;p53-dKO cerebellum compared to littermate controls. Scale bars = 200 μm (A) and 50 μm (B). **(I)** Fluorescent *in situ* hybridization using RNAScope probes against *Fgf5* mRNA (red) and DAPI labeling in the P0 Sufu;p53-dKO and control cerebellum. Boxed areas are enlarged to show ectopic localization of *Fgf5*+ cells in the EGL of the Sufu-p53-dKO cerebellum, unlike in controls. Scale bars = 200 μm and 50 μm (boxed area). **(J)** Double-immunofluorescence staining with Ki-67 (green) and phospho-Erk1/2 (pErk1/2; red) in the P0 Sufu;p53-dKO and control cerebelli. Boxed regions show cells double-labeled with pErk1/2+ and Ki-67+ cells in the control and Sufu;p53-dKO EGL Region B. Scale bars = 25 μm.

and precursor specification and differentiation defects (Kim et al., 2011, 2018; Jiwani et al., 2020; Yabut et al., 2020). Taken together, these findings indicate that SUFU acts at the intersection of SHH and FGF signaling to modulate GNP behavior (as summarized in our working model in **Fig. 5**). We postulate that SUFU exerts this role via stabilization of GLI transcription factors since we observed a decrease in GLI1, GLI2, and GLI3 protein level in the newborn Sufu-cKO cerebellum. Supporting this, Yin et al. (2019) found that reducing GLI2 levels rescued GNP hyperplasia and patterning defects in the Sufu-cKO neonatal cerebellum. Further studies are required to elucidate the involvement of GLI-dependent mechanisms in controlling *Fgf5* gene expression in the neonatal cerebellum.

In the wildtype cerebellum, *Fgf5*-expressing cells localize within the IGL surrounding the secondary fissure at P0 (**Fig. 4B**) (Ozawa et al., 1996; Hattori et al., 1997; Yaguchi et al., 2009) where GLI1 reporter activity (**Fig. 4A**), and SHH and PTCH1 expression are lowest (Corrales et al., 2004). By P4, *Fgf5* expression is detected in cells within the IGL throughout the cerebellum (Yaguchi et al., 2009). However, by P14, a time point at which most granule neurons have differentiated, *Fgf5* is no longer detected in the IGL or other cerebellar regions per Allen Developing Mouse Brain Atlas (Allen Institute for Brain Science, 2004). The strict spatiotemporal expression of *Fgf5* strongly supports a stage-specific role for regulating GNP development, particularly along the secondary fissure, to ensure timely differentiation and maturation of granule neurons. Indeed, as we observed in the P0 Sufu-cKO cerebellum, deregulation of *Fgf5* expression correlates with the continued uncontrolled proliferation of GNPs that have failed to differentiate normally. Follow-up studies geared towards characterizing cell-specific expression of *Fgf5* and how FGF5 acts on GNP differentiation are crucial to solidifying the exact function of FGF5 in early neonatal cerebellar development.

Our findings are contrary to previous reports of the proliferation-suppressive roles of FGFs, particularly FGF2, in GNPs specifically carrying *Ptch1* mutations (Fogarty et al., 2007; Emmenegger et al., 2013). However, in contrast to the Ptch1-cKO cerebellum, the newborn Sufu-cKO cerebellum still expresses PTCH1 and exhibits reduced GLI1, GLI2, and GLI3 protein levels (**Supplementary Fig. 1A**). These key molecular differences may activate unique signaling networks in Sufu-cKO GNPs. Additionally, 18 FGF ligands differ significantly in molecular features and binding specificities to distinct combinations of FGFR splice variants (Ornitz and Itoh, 2015). For example, unlike FGF2, which acts in an autocrine manner, FGF5 can exert both autocrine and paracrine functions, bind different combinations of FGFRs, and is dynamically expressed in distinct regions of the developing cerebellum. Thus, in-depth studies are needed to elucidate the exact mechanisms triggered by abnormally high levels of FGF5 in the developing cerebellum, particularly since *Fgf5* overexpression is known to drive cancer development and progression, including brain tumors (Allerstorfer et al., 2008). Importantly, examination of whether inhibition of FGF signaling by AZD4547 (or other FGFR inhibitors) in MB tumor-bearing Sufu;p53-dKO mice is crucial to establish that FGF signaling is a druggable target for SUFU-associated infantile MB^{SHH}.

The high occurrence of *SUFU* mutations in infantile MB indicates the selective vulnerability of the developing cerebellum to the neoplastic effects of SUFU dysfunction. Notably, the timing of *SUFU* LOF is critical; conditional deletion of *Sufu* in neural stem cells before granule neuron specification (using the hGFAP-Cre line) results in GNP hyperplasia, whereas conditional deletion of *Sufu* after granule neuron specification (using the Atoh1-Cre line) does not lead to these defects (Jiwani et al., 2020). Thus, *SUFU*-associated infantile MB^{SHH} is a likely consequence of defects stemming from the early stages of granule neuron lineage specification at embryonic stages. However, since hGFAP-Cre may also be expressed in cerebellar glial cells, we cannot yet eliminate the possibility that the defects are directly or indirectly a consequence of abnormal glial cell development and function. In-depth studies are required to interrogate the effects of SUFU LOF in cerebellar glial cell development and how this might indirectly affect GNP differentiation.

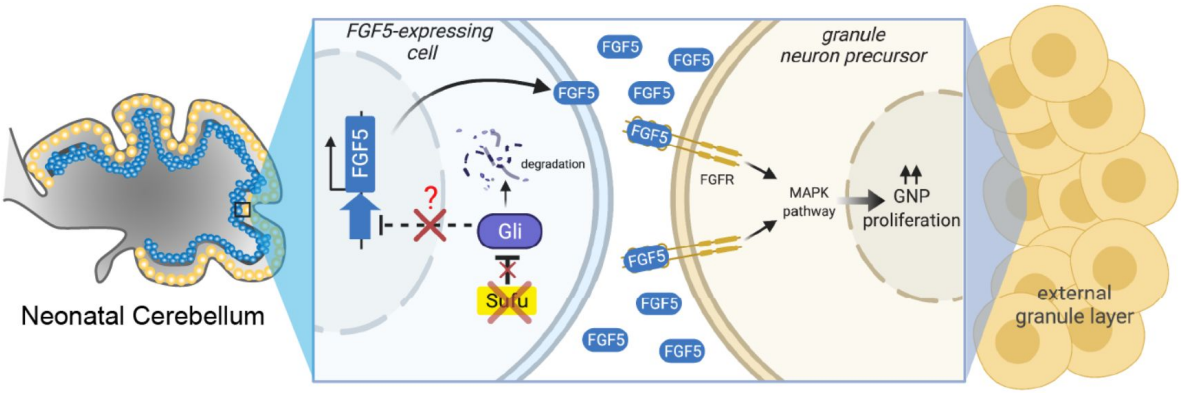

Figure 5

Loss of *Sufu* function drives excess proliferation of granule neuron precursors via FGF signaling activation.

The schematic diagram models how *Sufu* LOF facilitates the expansion of GNPs (yellow cells) in the EGL at the early stages of cerebellar development. We hypothesize that *Fgf5*-expressing cells (blue cells, yet to be identified) send FGF5 signal to GNP to proliferate and that ectopic expression of *Fgf5* in the absence of SUFU is responsible for the uncontrolled expansion of EGL localized GNPs.
Created with *BioRender.com/h05q807*.

Unfortunately, tumors initiated at embryonic stages are typically undetectable until several months after birth, when tumorigenesis has significantly progressed. Thus, therapeutics for infantile MB must successfully curtail tumorigenic mechanisms at postnatal stages and minimally affect normal GNPs elsewhere in the cerebellum. Towards this goal, inhibiting localized FGF5 and FGF signaling activity may provide new paths toward the design of targeted treatments. Since we confirmed the occurrence of high *FGF5* levels in a subset of infantile MB^{SHH} patients, measuring FGF5 may be a useful diagnostic biomarker for this patient population. This may predict the lack of efficacy of SHH-targeting compounds in curtailing tumor growth but could instead significantly impede cerebellar development. Importantly, detection of elevated FGF5 levels may identify patients who will be responsive to FGF-targeting treatments. Ultimately, we hope these studies facilitate the design of much-needed precision medicines to address the distinct oncogenic mechanisms specifically and effectively in infantile MB^{SHH} patients while enabling normal progression of cerebellar development.

Acknowledgements

We thank Hirofumi Noguchi and other members of the Pleasure Lab for critical discussions, the UCSF Center for Advanced Light Microscopy for assistance with imaging, and William Krause for assistance with transcriptomics. This work was supported by the NIH R01MH077694 and R01NS118995 (S.J.P.), R01MH077694-S1 (H.G.), NIH/NCI K01CA201068 (O.R.Y.), and American Brain Tumor Association Grant #A131363 (O.R.Y.).

This paper was typeset with the bioRxiv word template by @Chrelli: *www.github.com/chrelli/bioRxiv-word-template*.

Competing interest statement

The authors declare no competing financial interest.

Materials and Methods

Animals

Mice carrying the floxed *SUFU* allele ($Sufu^{fl}$) were kindly provided by Dr. Chi-Chung Hui (University of Toronto) and were genotyped as described elsewhere (Pospisilik et al., 2010). *hGFAP-cre* (Stock #004600; Schuller et al., 2008) and Gli1-LacZ (Stock #008211) mice were obtained from Jackson Laboratories (Bar Harbor, ME, USA). Mice designated as controls did not carry the *Cre* transgene and may have either one of the following genotypes: $Sufu^{fl/+}$ or $Sufu^{fl/fl}$. All mouse lines were maintained in mixed strains, and the analysis included male and female pups from each age group, although sex differences were not included in data reporting. All animal protocols were in accordance with National Institutes of Health regulations and approved by the UCSF Institutional Animal Care and Use Committee (IACUC).

In vivo treatment with FGFR inhibitor

The FGFR1-3 inhibitor, AZD4547 (Selleck Chemicals, #S2801), was dissolved sequentially in 4% Dimethyl Sulfoxide (DMSO), 30% Polyethylene glycol (PEG), 5% Tween-80, and water to make a 1mM solution. 1 µl of 1mM AZD4547, or vehicle only as control, was injected into the lateral

ventricle (~1 mm from the cerebellar midline) of pups for 5 days from P0/P1 using a 2.5 µl syringe (Model 62 RN; Hamilton Scientific). Pups remained with the mother until perfusion at P7 for analysis.

Immunohistochemistry and LacZ Staining

Perfusion, dissection, immunofluorescence, and LacZ staining were conducted according to standard protocols as previously described (Yabut et al., 2015). Briefly, P0/P1 brain tissues were fixed after dissection by direct immersion in 4% paraformaldehyde (PFA) overnight. P7 and older postnatal brains were fixed by intracardial perfusion with 4% PFA followed by two h post-fixation. All fixed brains were cryoprotected with a 15-30% sucrose gradient overnight before embedding in Optimal Cutting Temperature (OCT) compound for cryosectioning. Cryostat sections were air dried and rinsed 3× in PBS plus 0.2%Triton before blocking for 1 h in 10% normal lamb serum diluted in PBS with 0.2% Triton to prevent nonspecific binding. A heat-induced antigen retrieval protocol was performed on select immunohistochemistry experiments using 10 µM Citric Acid at pH 6.0. Primary antibodies were diluted in 10% serum in PBS with 0.2% Triton containing 4'6-diamidino-2-phenylindole (DAPI); sections were incubated in primary antibody overnight at room temperature. The following antibodies were used: rabbit anti-Pax6 (1:250 dilution; Cat. #: 901301, Biolegend); rabbit anti-NeuN (1:250 dilution; Cat. #: PA5-784-99, Invitrogen); mouse anti-Calretinin (1:250, Cat. #: AB5054, Millipore); rabbit anti-phospho-Erk1/2 (1:250 dilution; Cat. #: 4370, Cell Signaling); gH2AX (1:100 dilution; Cat. #: 05-636, Millipore); mouse anti-Ki-67 (1:100 dilution; Cat. #: 550809 BD Biosciences) and cleaved-Caspase 3 (1:250 dilution; Cat. #: 9661S, Cell Signaling). To detect primary antibodies, we used species-specific Alexa Fluor-conjugated secondary antibodies (1:500; Invitrogen) in 1X PBS-T for 1 h at room temperature, washed with 1X PBS, and coverslipped with Fluoromount-G (SouthernBiotech).

In Situ Hybridization

RNAScope ISH was conducted for *Fgf5* and *Ptch1*. RNAscope probes for Mm-*Fgf5* were designed commercially by the manufacturer (catalog # 417091, Advanced Cell Diagnostics, Inc.). RNAScope Assay was performed using the RNAscope Multiplex Fluorescent Reagent Kit V2 according to the manufacturer's instructions with the following conditions. Slides of cryosectioned brain tissues were prepared by air-drying for 30 minutes at 60ºC, then post-fixed in 4% PFA in 1X PBS for 15 minutes at 4ºC. Tissues were dehydrated at room temperature in an ethanol gradient (50% Ethanol, 70% Ethanol, then 100% ethanol) for 5 minutes each, followed by a final 100% ethanol wash for 5 minutes. RNAScope Hydrogen Peroxide treatment of tissues occurred for 10 minutes. Target retrieval was performed by immersing slides in RNAscope 1X Target Retrieval Reagent for 5 minutes in a 99ºC steamer. Tissue sections were subjected to RNAscope Protease Plus reagent treatment for 10-15 minutes at 40ºC in HybEZ Oven (ACDBio). Tissues were hybridized with the probe mix and incubated for 2 hours at 40ºC in the HybEZ Oven. AMP1, AMP2, and AMP3 sequential hybridization steps were performed as per manufacturer's instructions. Slides were incubated in RNAScope Multiplex FL v2 HRP-C1 for 15 minutes at 40ºC. Signals were detected using the TSA Plus Fluorescein Kit (catalog # NEL741E001KT, PerkinElmer) and Opal Dye reagent (Opal 570, catalog # FP1488001KT or Opal 520, catalog # FP1487001KT, from Akoya Biosciences) after 30 minutes of incubation at 40ºC.

Western Blot Analysis

Western blot analyses were conducted according to standard protocols. Soluble extracts were loaded onto Criterion, 4-15% Tris-HCI 4 SDS-PAGE gels (Bio-Rad), separated at 120V, and transferred to PVDF membrane at 30V for 2 hours or overnight at 4°C. Membranes were blocked with 3% milk/1X TBS-T (Tris-buffered saline with 0.1% Tween 20) or 5% BSA/1X TBS-T for 1hr at room temperature and incubated with primary antibodies diluted in blocking buffer overnight at 4°C, and secondary antibodies (1:5000 dilution; IR-Dye antibodies, LI-COR) for 1 hour at RT. Membranes were washed in 1X TBS-T and scanned using the Odyssey Infrared Imaging System (LI-

COR). Primary antibodies were used as follows: rabbit anti-Gli1 (1:1000; Abcam); goat anti-Gli2 (1:1000; R&D Systems), rabbit anti-Gli3 (1:100; Santa Cruz), rabbit anti-Pax6 (1:1000 dilution; Cat. #: 901301, Biolegend); rabbit anti-NeuN (1:1000 dilution; Cat. #: PA5-784-99, Invitrogen); rabbit anti-GABA A Receptor α6 (1:1000 dilution; Cat. #. PA5-77403, GABRA6; Invitrogen), and a-Tubulin (1:5000 dilution; Cat. #: ab4074, Abcam). Quantification and analysis were conducted using the Odyssey Image Studio Software (LI-COR). Protein levels were normalized to GAPDH protein levels. Levels of NeuN and GABRA6 were quantified in correlation with Pax6 levels (NeuN/Pax6 or GABRA6/Pax6) to determine the proportion of Pax6+ cells expressing mature granule neuron markers.

Image Analysis and Acquisition

Images were acquired using a Nikon E600 microscope equipped with a QCapture Pro camera (QImaging), Zeiss Axioscan Z.1 (Zeiss, Thornwood, NY, USA) using the Zen 2 blue edition software (Zeiss, Thornwood, NY, USA), or the Nikon Ti inverted microscope with CSU-W1 large field of view confocal and Andor Zyla 4.2 sCMOS camera. All images were imported in tiff or jpeg format. Brightness, contrast, and background were adjusted equally for the entire image between controls and mutants using the “Brightness/Contrast” and “Levels” functions from the “Image/Adjustment” options in Adobe Photoshop or NIH ImageJ without any further modification. NIH Image J was used to threshold background levels between controls and mutant tissues to quantify fluorescence labeling. To quantify cell density, positively labeled cells within defined EGL regions, as defined in **Fig. 2A**, were counted. Quantification of double-labeled cells was performed in 1-2 mm optical slices obtained by confocal microscopy. We relied on continuous DAPI nuclear staining to distinguish individual cells in each optical slice to determine the cellular colocalization of specific markers being analyzed (e.g., pERK and Ki-67). All measurements were performed from 2-3 20 mm thick and histologically matched cerebellar sections of 3-6 independent mice per genotype analyzed. Individual points in the bar graphs represent the average cell number (quantified from 2-3 sections) from each mouse.

Human MB Gene Expression

Expression values of FGF5 (ENSG00000138675) were assessed using Geo2R (Barrett et al., 2013) from published human MB subtype expression dataset accession no. GSE85217 (Cavalli et al., 2017). GEO2R is an interactive web tool that compares expression levels of genes of interest (GOI) between sample groups in the GEO series using original submitter-supplied processed data tables. We entered the GOI Ensembl ID and organized data sets according to age and MB subgroup or MB^{SHH} subtype classifications. GEO2R results presented gene expression levels as a table ordered by FDR-adjusted (Benjamini & Hochberg) p-values, with significance level cut-off at 0.05, processed by GEO2R’s built-in limma statistical test. The resulting data were subsequently exported into Prism (GraphPad). Scatter plots presenting FGF5 expression levels across all MB subgroups (**Figure 1A**) and MB^{SHH} subtypes (**Figure 1D**). We performed additional statistical analyses to compare FGF5 expression levels between MB subgroups and MB^{SHH} subtypes and graphed these data as violin plots (**Figure 1B, 1C**, and **1E**). For these analyses, we used one-way ANOVA with Holm-Sidak’s multiple comparisons test, single pooled variance. *P* value ≤0.05 was considered statistically significant. Graphs display the mean ± standard error of the mean (SEM). Sample sizes analyzed were: MB^{WNT} n=70, MB^{SHH} n=224, MB^{GR3} n=143, MB^{GR4} n=326, MB^{SHHa} n=66, MB^{SHHb} n=35, MB^{SHHg} n=47, and MB^{SHHd} n=76.

Statistics

Prism 8.1 (GraphPad) was used for statistical analysis. Two sample experiments were analyzed by Student’s *t* test, and experiments with more than two parameters were analyzed by ANOVA. In 1-or 2-way ANOVA, when interactions were found, follow-up analyses were conducted for the relevant variables using Holm-Sidak’s multiple comparisons test. All experiments were conducted at least

in triplicate with sample sizes of n = 3–6 embryos/animals/slices per genotype. *P* value ≤0.05 was considered statistically significant. Graphs display the mean ± standard error of the mean (SEM). Statistical values and analyses are summarized in Table 1.

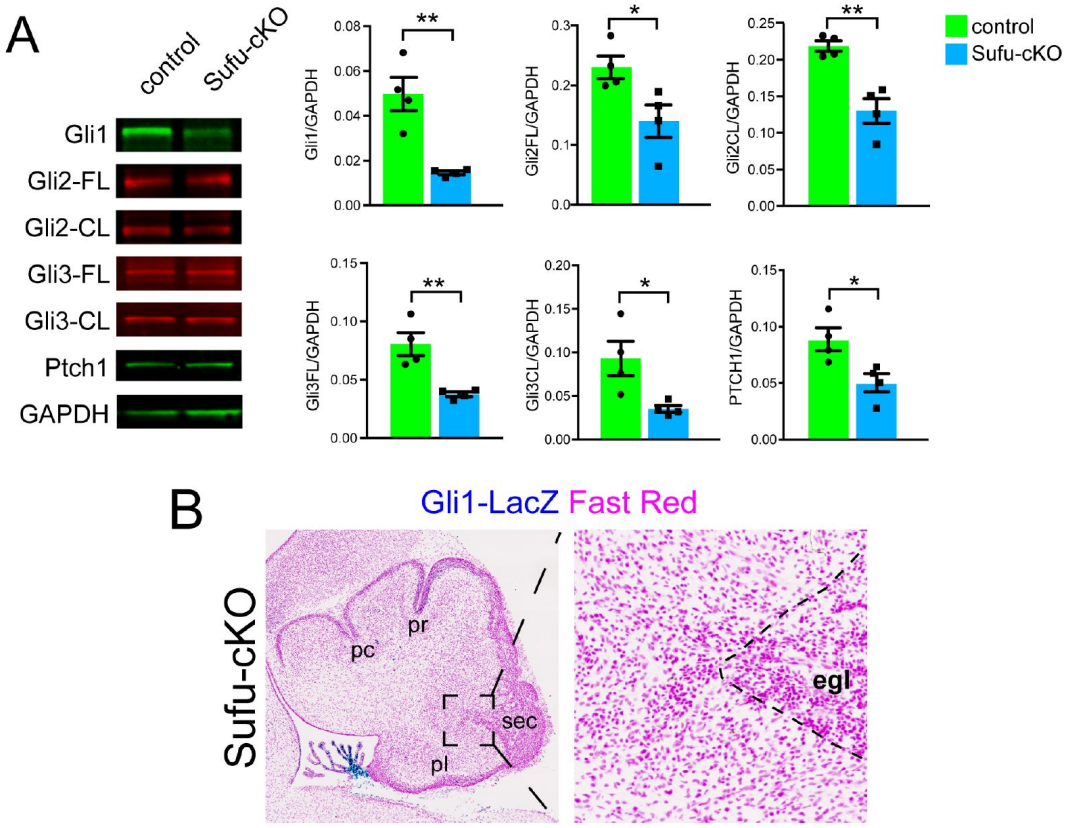

Supplementary Figure 1

Reduced SHH signaling activity in the P0 Sufu-cKO cerebellum.

(A) Western blot analysis of cerebellar protein lysates from P0 control and Sufu-cKO mice showing significantly lower levels of total and cleaved versions of Gli transcription factors in the P0 Sufu-cKO cerebellum. *p<0.05, **p<0.01 (**B)** b-galactosidase activity (blue), representing the Gli1-LacZ transgene, is largely absent in areas adjacent to the EGL along the secondary (sec) fissure of the P0 Sufu-cKO cerebellum.

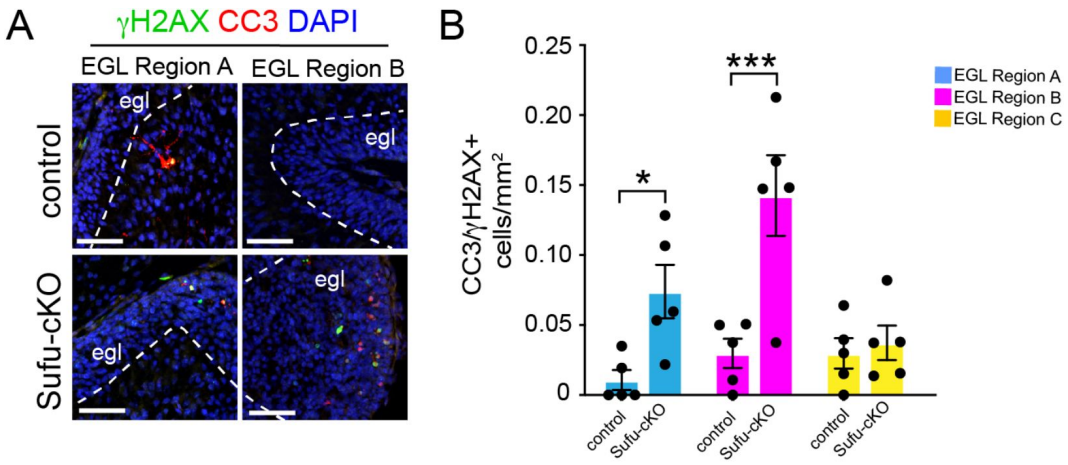

Supplementary Figure 2

Evidence of pre-neoplastic lesions and high rates of cell death in Sufu-cKO granule neuron precursors.

(A) Double-immunofluorescence staining with (γH2AX (green) and cleaved-caspase 3 (CC3; red), a marker for apoptotic cells, and DAPI labeling in regions A and B. Scale bars = 50 μm **(B)** Quantification of the density of cells labeled with CC3 and (γH2AX within each EGL regions. *p<0.05, ***p<0.001.

References

Allen Institute for Brain Science (2004) **Allen Mouse Brain Atlas [dataset]**

Allerstorfer S *et al.* (2008) **FGF5 as an oncogenic factor in human glioblastoma multiforme: autocrine and paracrine activities** *Oncogene* **27**:4180–4190

Bai C. B., Auerbach W., Lee J. S., Stephen D., Joyner A. L. (2002) **Gli2, but not Gli1, is required for initial Shh signaling and ectopic activation of the Shh pathway** *Development* **129**:4753–4761

Barrett T *et al.* (2013) **NCBI GEO: archive for functional genomics data sets--update** *Nucleic acids research* **41**:D991–5

Cavalli FMG, et al. (2017) **Intertumoral Heterogeneity within Medulloblastoma Subgroups** *Cancer Cell* **31**:737–754

Chen M-H, Wilson CW, Li Y-J, Law KK Lo, Lu C-S, Gacayan R, Zhang X, Hui C, Chuang P-T (2009) **Cilium-independent regulation of Gli protein function by Sufu in Hedgehog signalling is evolutionarily conserved** *Genes & development* **23**:1910–1928

Clements DA, Wang JK, Dionne CA, Goldfarb M (1993) **Activation of fibroblast growth factor (FGF) receptors by recombinant human FGF-5** *Oncogene* **8**:1311–1316

Corrales JD, Rocco GL, Blaess S, Guo Q, Joyner AL (2004) **Spatial pattern of sonic hedgehog signaling through Gli genes during cerebellum development** *Development* :5581–5590

Emmenegger BA *et al.* (2013) **Distinct roles for fibroblast growth factor signaling in cerebellar development and medulloblastoma** *Oncogene* **32**:4181–4188

Fogarty MP, Emmenegger BA, Grasfeder LL, Oliver TG, Wechsler-Reya RJ, Lefkowitz RJ (2007) **Fibroblast growth factor blocks Sonic hedgehog signaling in neuronal precursors and tumor cells** *PNAS* **104**:2973–2978

Gao Y, Ferguson DO, Xie W, Manis JP, Sekiguchi J, Frank KM, Chaudhuri J, Horner J, DePinho RA, Alt FW (2000) **Interplay of p53 and DNA-repair protein XRCC4 in tumorigenesis, genomic stability and development** *Nature* **404**:897–900

Gudernova I *et al.* (2016) **Multikinase activity of fibroblast growth factor receptor (FGFR) inhibitors SU5402, PD173074, AZD1480, AZD4547 and BGJ398 compromises the use of small chemicals targeting FGFR catalytic activity for therapy of short-stature syndromes** *Human Molecular Genetics* **25**:9–23

Guerrini-Rousseau L, et al. (2018) **Germline SUFU mutation carriers and medulloblastoma: clinical characteristics, cancer risk, and prognosis** *Neuro-Oncology* **20**:1122–1132

Hattori Y, Miyake A, Mikami T, Ohta M, Itoh N (1997) **Transient expression of FGF-5 mRNA in the rat cerebellar cortex during post-natal development** *Molecular Brain Research* **47**:262–266

Jiwani T, Kim JJ, Rosenblum ND (2020) **Suppressor of fused controls cerebellum granule cell proliferation by suppressing Fgf8 and spatially regulating Gli proteins** *Development* **147**

Kim JJ, Gill PS, Rotin L, van Eede M, Henkelman RM, Hui C-C, Rosenblum ND (2011) **Suppressor of fused controls mid-hindbrain patterning and cerebellar morphogenesis via GLI3 repressor** *Journal of Neuroscience* **31**:1825–1836

Kim JJ, Jiwani T, Erwood S, Loree J, Rosenblum ND (2018) **Suppressor of fused controls cerebellar neuronal differentiation in a manner modulated by GLI3 repressor and Fgf15** *Developmental Dynamics* **247**:156–169

Kong JH, Siebold C, Rohatgi R (2019) **Biochemical mechanisms of vertebrate hedgehog signaling** *Development* **146**

Kool M, et al. (2014) **Genome Sequencing of SHH Medulloblastoma Predicts Genotype-Related Response to Smoothened Inhibition** *Cancer Cell* **25**:393–405

Leto K, et al. (2016) **Consensus Paper: Cerebellar Development** *The Cerebellum* **15**:789–828

Lin C, Chen M-H, Yao E, Song H, Gacayan R, Hui C, Chuang P-T (2014) **Differential regulation of Gli proteins by Sufu in the lung affects PDGF signaling and myofibroblast development** *Developmental biology* **392**:324–333

Mah L-J, El-Osta A, Karagiannis TC (2010) **γH2AX: a sensitive molecular marker of DNA damage and repair** *Leukemia* **24**:679–686

Marino S, Vooijs M, van Der Gulden H, Jonkers J, Berns A (2000) **Induction of medulloblastomas in p53-null mutant mice by somatic inactivation of Rb in the external granular layer cells of the cerebellum** *Genes & development* **14**:994–1004

Matise MP, Wang H (2011) **Sonic hedgehog signaling in the developing CNS where it has been and where it is going** *Current topics in developmental biology* **97**:75–117

Ornitz DM, Itoh N (2015) **The Fibroblast Growth Factor signaling pathway** *Wiley interdisciplinary reviews Developmental biology* **4**:215–266

Ornitz DM, Xu J, Colvin JS, McEwen DG, MacArthur CA, Coulier F, Gao G, Goldfarb M (1996) **Receptor specificity of the fibroblast growth factor family** *The Journal of biological chemistry* **271**:15292–15297

Ostrom QT, Gittleman H, Xu J, Kromer C, Wolinsky Y, Kruchko C, Barnholtz-Sloan JS (2016) **CBTRUS Statistical Report: Primary Brain and Other Central Nervous System Tumors Diagnosed in the United States in 2009–2013** *Neuro-Oncology* **18**:v1–v75

Ozawa K, Uruno T, Miyakawa K, Seo M, Imamura T (1996) **Expression of the fibroblast growth factor family and their receptor family genes during mouse brain development** *Molecular Brain Research* **41**:279–288

Pospisilik JA, et al. (2010) **Drosophila genome-wide obesity screen reveals hedgehog as a determinant of brown versus white adipose cell fate** *Cell* **140**:148–160

Schwalbe EC *et al.* (2017) **Novel molecular subgroups for clinical classification and outcome prediction in childhood medulloblastoma: A cohort study** *The Lancet Oncology* **18**:958–971

Schüller U. *et al.* (2008) **Acquisition of granule neuron precursor identity is a critical determinant of progenitor cell competence to form Shh-induced medulloblastoma** *Cancer Cell* **14**:123–134

Tan I-L *et al.* (2018) **Lateral cerebellum is preferentially sensitive to high sonic hedgehog signaling and medulloblastoma formation** *Proceedings of the National Academy of Sciences of the United States of America* **115**:3392–3397

Vanner RJ, et al. (2014) **Quiescent Sox2+ Cells Drive Hierarchical Growth and Relapse in Sonic Hedgehog Subgroup Medulloblastoma** *Cancer Cell* **26**:33–47

Vladoiu MC, et al. (2019) **Childhood cerebellar tumours mirror conserved fetal transcriptional programs** *Nature* **572**:67–73

Wang C, Pan Y, Wang B (2010) **Suppressor of fused and Spop regulate the stability, processing and function of Gli2 and Gli3 full-length activators but not their repressors** *Development* :2001–2009

Ward E, DeSantis C, Robbins A, Kohler B, Jemal A (2014) **Childhood and adolescent cancer statistics, 2014** *CA: A Cancer Journal for Clinicians* **64**:83–103

Yabut OR, Fernandez G, Huynh T, Yoon K, Pleasure SJ (2015) **Suppressor of Fused Is Critical for Maintenance of Neuronal Progenitor Identity during Corticogenesis** *Cell Reports* **12**:2021–2034

Yabut OR, Ng H-X, Yoon K, Arela JC, Ngo T, Pleasure SJ (2020) **The neocortical progenitor specification program is established through combined modulation of SHH and FGF signaling** *The Journal of Neuroscience* **40**:6872–6887

Yaguchi Y, Yu T, Ahmed MU, Berry M, Mason I, Basson MA (2009) **Fibroblast growth factor (FGF) gene expression in the developing cerebellum suggests multiple roles for FGF signaling during cerebellar morphogenesis and development** *Developmental Dynamics* **238**:2058–2072

Yin W-C, et al. (2019) **Dual Regulatory Functions of SUFU and Targetome of GLI2 in SHH Subgroup Medulloblastoma** *Developmental Cell* **48**:167–183

Yu T, Yaguchi Y, Echevarria D, Martinez S, Basson MA (2011) **Sprouty genes prevent excessive FGF signalling in multiple cell types throughout the development of the cerebellum** *Development* **138**:2957–2968

Zhuo L, Theis M, Alvarez-Maya I, Brenner M, Willecke K, Messing A (2001) **hGFAP-cre transgenic mice for manipulation of glial and neuronal function in vivo** *Genesis* **31**:85–94

Author information

Odessa R Yabut

Department of Neurology, Weill Institute for Neuroscience, University of California San Francisco, San Francisco, United States
ORCID iD: 0000-0001-9991-0167

For correspondence: oryabut@gmail.com

Hector Gomez
Department of Neurology, Weill Institute for Neuroscience, University of California San Francisco, San Francisco, United States
ORCID iD: 0000-0002-8894-0093

Jessica Arela
Department of Neurology, Weill Institute for Neuroscience, University of California San Francisco, San Francisco, United States
ORCID iD: 0000-0002-5748-2958

Jesse Garcia Castillo
Department of Neurology, Weill Institute for Neuroscience, University of California San Francisco, San Francisco, United States

Thomas Ngo
Department of Neurology, Weill Institute for Neuroscience, University of California San Francisco, San Francisco, United States, Department of Psychiatry, Weill Institute for Neuroscience, University of California San Francisco, San Francisco, United States
ORCID iD: 0000-0003-2504-1872

Samuel J Pleasure
Department of Neurology, Weill Institute for Neuroscience, University of California San Francisco, San Francisco, United States, Programs in Neuroscience and Developmental Biology, Eli and Edythe Broad Center of Regeneration Medicine and Stem Cell Research, University of California San Francisco, San Francisco, United States
ORCID iD: 0000-0001-8599-1613

For correspondence: samuel.pleasure@ucsf.edu

Editors

Reviewing Editor
Joshua Corbin
Children's National Hospital, Washington, United States of America

Senior Editor
Jonathan Cooper
Fred Hutchinson Cancer Research Center, Seattle, United States of America

Reviewer #1 (Public review):

Summary:

SUFU modulates Sonic hedgehog (SHH) signaling and is frequently mutated in the B-subtype of SHH driven medulloblastoma. The B-subtype occurs mostly in infants, is often metastatic, and lacks specific treatment. Yabut et al. found Fgf5 was highly expressed in the B-subtype of SHH driven medulloblastoma by examining a published microarray expression dataset. They then investigated how Fgf5 functions in the cerebellum of mice that have embryonic Sufu loss of function. This loss was induced using the hGFAP-cre transgene, which is expressed multiple cell types in the developing cerebellum, including granule neuron precursors (GNPs)

derived from the rhombic lip. By measuring the area of Pax6+ cells in the external granule cell layer (EGL) of Sufu-cKO mice at postnatal day 0, they find Pax6+ cells occupy a larger area in the posterior lobe adjacent to the secondary fissure, which is poorly defined. They show that Fgf5 RNA and phosphoErk1/2 immunostaining are also higher in the same disrupted region. Some of the phosphoErk1/2+ cells are proliferative in the Sufu-cKO. Western blot analysis of Gli proteins that modulate SHH signaling found reduced expression and absence of Gli1 activity in the region of cerebellar dysgenesis in Sufu-cKO mice. This suggests the GNP expansion in this region is independent of SHH signaling. Amazingly, intraventricular injection of the FGFR1-2 antagonist AZD4547 from P0-4 and examined histologoically at P7 found the treatment restored cytoarchitecture in the cerebella of Sufu-cKO mice. This is further supported by NeuN immunostaining in the internal granule cell layer, which labels mature, non-diving neurons, and KI67 immunostaining, indicating dividing cells, and primarily found in the EGL. The mice were treated beginning at a timepoint when cerebellar cytoarchitecture was shown to be disrupted and it is indistinguishable from control following treatment. Fig.3 presents the most convincing and exciting data in this manuscript.

Sufu-cKO do not readily develop cerebellar tumors. The authors detected phosphorylated H2AX immunostaining, which labels double strand breaks, was in some cells in the EGL in regions of cerebellar dysgenesis in the Sufu-cKO, as was cleaved Caspase 3, a marker of apoptosis. P53, downstream of the double strand break pathway, protein was reduced in Sufu-cKO cerebellum. Genetically removing p53 from the Sufu-cKO cerebellum resulted in cerebellar tumors in 2 mo mice. The Sufu;p53-dKO cerebella at P0 lacked clear foliation, and the secondary fissure, even more so than the Sufu-cKO. Fgf5 RNA and signaling (pERK1/2) were also expressed ectopically.

In the revised manuscript, additional details have been added to clarify statistical analyses and to state limitations of the reported results in the absence of further experimental analyses.

https://doi.org/10.7554/eLife.100767.2.sa3

Reviewer #2 (Public review):

Summary:

Mutations in SUFU are implicated in SHH medulloblastoma (MB). SUFU modulates Shh signaling in a context-dependent manner, making its role in MB pathology complex and not fully understood. This study reports that elevated FGF5 levels are associated with a specific subtype of SHH MB, particularly in pediatric cases. The authors demonstrate that Sufu deletion in a mouse model leads to abnormal proliferation of granule cell precursors (GCPs) at the secondary fissure (region B), correlating with increased Fgf5 expression. Notably, pharmacological inhibition of FGFR restores normal cerebellar development in Sufu mutant mice.

Strengths:

The identification of increased FGF5 in subsets of MB is novel and a key strength of the paper.

Weaknesses:

The study appears incomplete despite the potential significance of these findings. The current paper does not fully establish the causal relationship between Fgf5 and abnormal cerebellar development, nor does it clarify its connection to SUFU-related MB. Some conclusions seem overstated, and the central question of whether FGFR inhibition can prevent tumor formation remains untested.

Comments on revisions:

In this revised version, many of the concerns and comments raised by this and other reviewers remain unaddressed and require attention in future studies. The manuscript does not demonstrate significant improvement.

Specific Comments:

(1) In the figure provided by the authors, FGF5 appears to be highly expressed beneath the GCPs. Regarding our comment and Reviewer 1's Comment 7, it is essential to identify the cell types secreting FGF5 and clarify whether it functions in a paracrine or autocrine manner. This should be incorporated into the working model illustrated in Figure 5.
(2) Contrary to the authors' claim that their results align completely with Jiwani et al. (2020), there is a discrepancy in the data. Jiwani et al. reported an increase in Gli2 levels in the Sufu mutant, whereas the current study shows the opposite result. This inconsistency needs to be addressed.

https://doi.org/10.7554/eLife.100767.2.sa2

Reviewer #3 (Public review):

Summary:

The interaction between FGF signaling and SHH-mediated GNP expansion in MB, particularly in the context of Sufu LoF, has just begun to be understood. The manuscript by Yabut et al. establishes a connection between ectopic FGF5 expression and GNP over-expansion in a late stage embryonic Sufu LoF model. The data provided links region-specific interaction between aberrant FGF5 signaling with SHH subtype of medulloblastoma. New data from Yabut et al. suggest that ectopic FGF5 expression correlates with GNP expansion near the secondary fissure in Sufu LoF cerebella. Furthermore, pharmacological blockade of FGF signaling inhibits GNP proliferation. Interestingly, the data indicate that the timing of conditional Sufu deletion (E13.5 using the hGFAP-Cre line) results in different outcomes compared to later deletion (using Math1-cre line, Jiwani et al., 2020). This study provides significant insights into the molecular mechanisms driving GNP expansion in SHH subgroup MB, particularly in the context of Sufu LoF. It highlights the potential of targeting FGF5 signaling as a therapeutic strategy. Additionally, the research offers a model for better understanding MB subtypes and developing targeted treatments.

Strengths:

One notable strength of this study is the extraction and analysis of ectopic FGF5 expression from a subset of MB patient tumor samples. This translational aspect of the study enhances its relevance to human disease. By correlating findings from mouse models with patient data, the authors strengthen the validity of their conclusions and highlight the potential clinical implications of targeting FGF5 in MB therapy.

The data convincingly show that FGFR signaling activation drives GNP proliferation in Sufu conditional knockout models. This finding is supported by robust experimental evidence, including pharmacological blockade of FGF signaling, which effectively inhibits GNP proliferation. The clear demonstration of a functional link between FGFR signaling and GNP expansion underscores the potential of FGFR as a therapeutic target in SHH subgroup medulloblastoma.

Previous studies have demonstrated the inhibitory effect of FGF2 on tumor cell proliferation in certain MB types, such as the ptc mutant (Fogarty et al., 2006)(Yaguchi et al., 2009).

Findings in this manuscript provide additional support suggesting multiple roles for FGF signaling in cerebellar patterning and development.

Weaknesses:

In the GEO dataset analysis, where FGF5 expression is extracted, the reporting of the P-value lacks detail on the statistical methods used, such as whether an ANOVA or t-test was employed. Providing comprehensive statistical methodologies is crucial for assessing the rigor and reproducibility of the results. The absence of this information raises concerns about the robustness of the statistical analysis.

Another concern is related to the controls used in the study. Cre recombinase induces double-strand DNA breaks within the loxP sites, and the control mice did not carry the Cre transgene (as stated in the Method section), while Sufu-cKO mice did. This discrepancy necessitates an additional control group to evaluate the effects of Cre-induced double-strand breaks on phosphorylated H2AX-DSB signaling. Including this control would strengthen the validity of the findings by ensuring that observed effects are not artifacts of Cre recombinase activity.

Although the use of the hGFAP-Cre line allows genetic access to late embryonic stage, this also targets multiple cell types, including both GNPs and cerebellar glial cells. However, the authors focus primarily on GNPs without fully addressing the potential contributions of neuron-glial interaction. This oversight could limit the understanding of the broader cellular context in which FGF signaling influences tumor development.

- Statistical analysis from the Geo expression dataset:
The reviewer is satisfied with the revisions provided by the author and considers Figure 1 substantially improved.

- Generation of Sufu-cKO;Gli1-LacZ triple transgenic mice not described:
>The reviewer finds that the supplementary Figure 1 revisions provided by the author do not fully address the concerns raised, and the issue remains unresolved.

- Request control group to evaluate the effects of Cre induced double-strand breaks on phosphorylated H2AX-DSB signaling:
>Despite the revisions, control group (hGFAPCre;Sufu-fl/+) highlighted in the author response does not present in the revision, leaving this issue unresolved.

- hGFAP-Cre line also targets multiple celltypes, including both GNPs and cerebellar glial cells:
>The author acknowledges the limitations of the study, and the reviewer concurs, noting that it enhances the contextual understanding of the findings.

https://doi.org/10.7554/eLife.100767.2.sa1

Author response:

The following is the authors' response to the original reviews.

> *The reviewers suggest a number of experiments and re-analyses to strengthen their claims and enhance the impact of the study. While a number of these are longer term, below is a summary of experiments and analyses recommended by the reviewers that can be accomplished in the shorter term:*
>
> *(1) Clarification of statistical approaches, quantification, data presentation and description of cerebellar anatomical nomenclature (e.gs. detailed statistical methods for the GEO dataset analysis, FDR correction, quantification in Figs 2-4)*

The revised manuscript will provide detailed statistical methods including FDR correction for GEO dataset analyses and quantification. Please see specific responses to GEO dataset analyses below.

> *(2) Improved quality of images for select immunostains and in situ hybridization*

The revised manuscript will address the quality of the images as indicated by the reviewers.

> *(3) Include a control group of hGFAP-Cre mice with loxP sites but without Sufu deletion to assess the effects of Cre-induced double-strand breaks on phosphorylated H2AX-DSB signaling.*

The breeding scheme we used to generate homozygous SUFU conditional mutants will not generate pups carrying only hGFAP-Cre. Thus, we are unable to compare expression of gH2AX expression in littermates that do not carry loxP sites. The reviewer is correct in pointing out the possibility of Cre recombinase activity inducing double-strand breaks on its own. However, it is likely that any hGFAP-Cre induced double-strand breaks does not sufficiently cause the phenotypes we observed in homozygous mutants (Sufu-cKO) mice because the cerebellum of mice carry heterozygous SUFU mutations (hGFAP-Cre;Sufu-fl/+) do not display the profound cerebellar phenotypes observed in Sufu-cKO mice. We cannot rule out, however, any undetectable abnormalities that could be present which may require further analyses.

> ***Public Reviews:***
>
> ***Reviewer #1 (Public Review):***
>
> *Summary:*
>
> *SUFU modulates Sonic hedgehog (SHH) signaling and is frequently mutated in the B-subtype of SHH-driven medulloblastoma. The B-subtype occurs mostly in infants, is often metastatic, and lacks specific treatment. Yabut et al. found that Fgf5 was highly expressed in the B-subtype of SHH-driven medulloblastoma by examining a published microarray expression dataset. They then investigated how Fgf5 functions in the cerebellum of mice that have embryonic Sufu loss of function. This loss was induced using the hGFAP-cre transgene, which is expressed in multiple cell types in the developing cerebellum, including granule neuron precursors (GNPs) derived from the rhombic lip. By measuring the area of Pax6+ cells in the external granule cell layer (EGL) of Sufu-cKO mice at postnatal day 0, they find Pax6+ cells occupy a larger area in the posterior lobe adjacent to the secondary fissure, which is poorly defined. They show that Fgf5 RNA and phosphoErk1/2 immunostaining are also higher in the same disrupted region. Some of the phosphoErk1/2+ cells are proliferative in the Sufu-cKO. Western blot analysis of Gli proteins that modulate SHH signaling found reduced expression and absence of Gli1 activity in the region of cerebellar dysgenesis in Sufu-cKO mice. This suggests the GNP expansion in this region is independent of SHH signaling. Amazingly, intraventricular injection of the FGFR1-2 antagonist AZD4547 from P0-4 and examined histologically at P7 found the treatment restored cytoarchitecture in the cerebella of Sufu-cKO mice. This is further supported by NeuN immunostaining in the internal granule cell layer, which labels mature, non-diving neurons, and KI67 immunostaining, indicating dividing cells, and primarily found in the EGL. The mice were treated beginning at a timepoint when cerebellar cytoarchitecture was shown to be disrupted and it is indistinguishable from control following treatment. Figure 3 presents the most convincing and exciting data in this manuscript.*

Sufu-cKO do not readily develop cerebellar tumors. The authors detected phosphorylated H2AX immunostaining, which labels double-strand breaks, in some cells in the EGL in regions of cerebellar dysgenesis in the Sufu-cKO, as was cleaved Caspase 3, a marker of apoptosis. P53, downstream of the double-strand break pathway, the protein was reduced in Sufu-cKO cerebellum. Genetically removing p53 from the Sufu-cKO cerebellum resulted in cerebellar tumors in 2-month old mice. The Sufu;p53-dKO cerebella at P0 lacked clear foliation, and the secondary fissure, even more so than the Sufu-cKO. Fgf5 RNA and signaling (pERK1/2) were also expressed ectopically.

The conclusions of the paper are largely supported by the data, but some data analysis need to be clarified and extended.

(1) The rationale for examining Fgf5 in medulloblastoma is not sufficiently convincing. The authors previously reported that Fgf15 was upregulated in neocortical progenitors of mice with conditional loss of Sufu (PMID: 32737167). In Figure 1, the authors report FGF5 expression is higher in SHH-type medulloblastoma, especially the beta and gamma subtypes mostly found in infants. These data were derived from a genome-wide dataset and are shown without correction for multiple testing, including other Fgfs. Showing the expression of other Fgfs with FDR correction would better substantiate their choice or moving this figure to later in the manuscript as support for their mouse investigations would be more convincing.

To assess FGF5 (ENSG00000138675) expression in MB tissues, we used Geo2R (Barrett et al., 2013) to analyze published human MB subtype expression arrays from accession no. GSE85217 (Cavalli et al., 2017). GEO2R is an interactive web tool that compares expression levels of genes of interest (GOI) between sample groups in the GEO series using original submitter-supplied processed data tables. We entered the GOI Ensembl ID and organized data sets according to age and MB subgroup or MB^{SHH} subtype classifications. GEO2R results presented gene expression levels as a table ordered by FDR-adjusted (Benjamini & Hochberg) p-values, with significance level cut-off at 0.05, processed by GEO2R's built-in limma statistical test. Resulting data were subsequently exported into Prism (GraphPad). We generated scatter plots presenting FGF5 expression levels across all MB subgroups (Figure 1A) and MB^{SHH} subtypes (Figure 1D). We performed additional statistical analyses to compare FGF5 expression levels between MB subgroups and MB^{SHH} subtypes and graphed these data as violin plots (Figure 1B, 1C, and 1E). For these analyses, we used one-way ANOVA with Holm-Sidak's multiple comparisons test, single pooled variance. *P* value ≤0.05 was considered statistically significant. Graphs display the mean ± standard error of the mean (SEM).

Author response image 1.

Comparative expression of FGF ligands, FGF5, FGF10, FGF12, and FGF19, across all MB subgroups. FGF12 expression is not significantly different, while FGF5, FGF10, and FGF19, show distinct upregulation in MB^{SHH} subgroup (MB^{WNT} n=70, MB^{SHH} n=224, MB^{GR3} n=143, MB^{GR4} n=326).

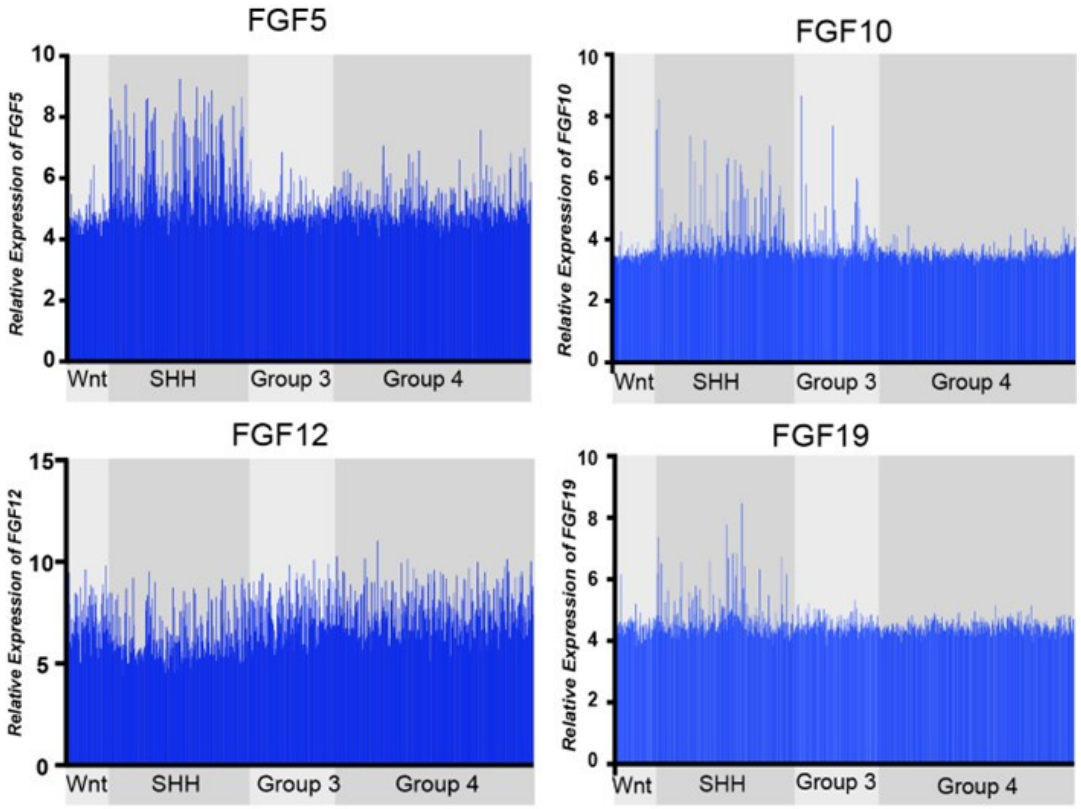

Expression of the 21 known FGF ligands were also analyzed. Many FGFs did not exhibit differential expression levels in MB^{SHH} compared to other MB subgroups, such as with FGF12 in Figure 1. FGF5, FGF10, and FGF19 (the human orthologue of mouse FGF15) all showed specific upregulation in MB^{SHH} compared to other MB subgroups (Author response image 1), supporting our previous observations that FGF15 is a downstream target of SHH signaling (Yabut et al., 2020), as the reviewer pointed out. However, further stratification of MB^{SHH} patient data revealed that only FGF5 specifically showed upregulation in infants with MBSHH ($MB^{SHH\beta}$ and $MB^{SHH\gamma}$ Author response image 2) indicating a more prominent role for FGF5 in the developing cerebellum and driver of MB^{SHH} tumorigenesis in this dynamic environment.

Author response image 2.

Comparative expression of FGF5, FGF10, and FGF19 in different MB^{SHH} subtypes. FGF5 specifically show mRNA relative levels above 6 in 81% of MB^{SHH} infant patient tumors (n=80 $MB^{SHH\alpha}$ and $MB^{SHH\gamma}$ tumors) unlike 35% of $MB^{SHH\alpha}$ (n=65) or 0% of $MB^{SHH\delta}$ (n=75) tumors.

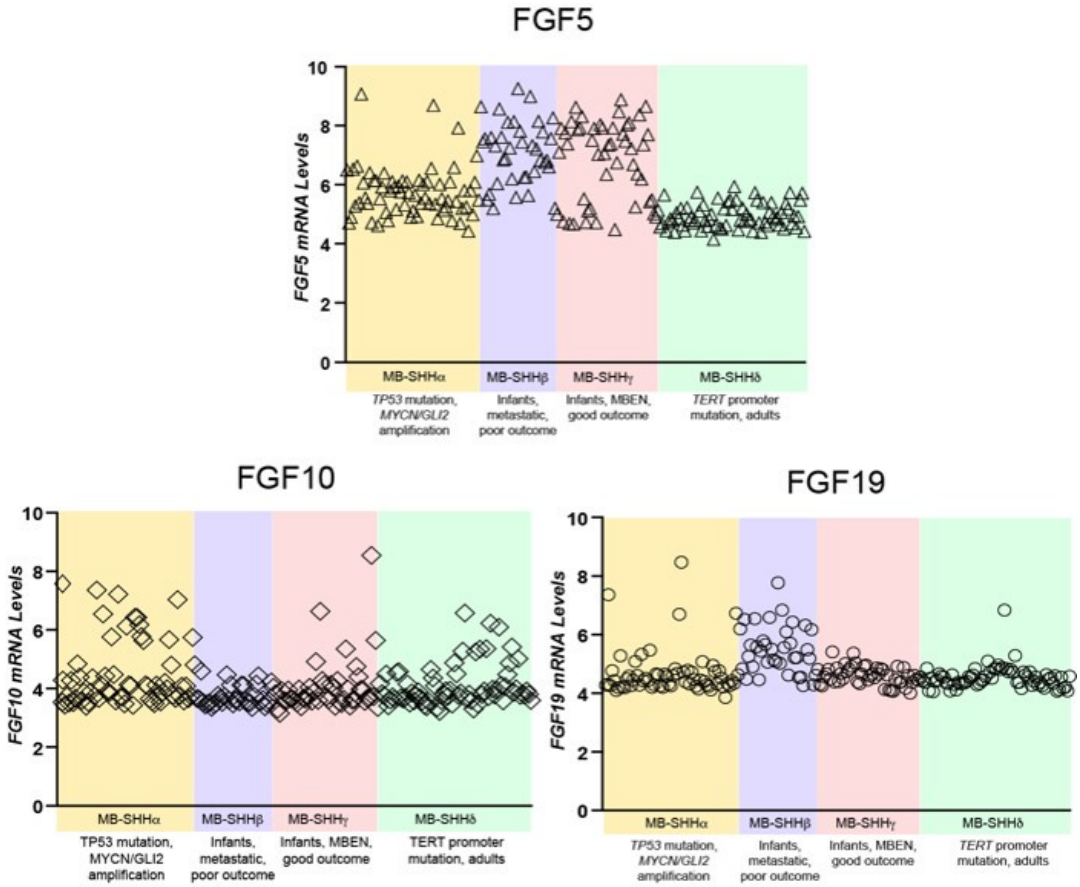

> *(2) The Sufu-cKO cerebellum lacks a clear anchor point at the secondary fissure and foliation is disrupted in the central and posterior lobes. It would be helpful for the authors to review Sudarov & Joyner (PMID: 18053187) for nomenclature specific to the developing cerebellum.*

The reviewers are correct that the cerebellar foliation is severely disrupted in central and posterior lobes, as per Sudarov and Joyner (Neural Development 2007). This nomenclature may be referred to describe the regions referred in this manuscript.

> *(3) The metrics used to quantify cerebellar perimeter and immunostaining are not sufficiently described. It is unclear whether the individual points in the bar graph represent a single section from independent mice, or multiple sections from the same mice. For example, in Figures 2B-D. This also applies to Figure 3C-D.*

All quantification were performed from 2-3 20 um cerebellar sections of 3-6 independent mice per genotype analyzed. Individual points in the bar graphs represent the average cell number (quantified from 2-3 sections) from each mice. Figure 2B show data points from n=4 mice per genotype. Figure 2C show data from n=3 mice per genotype. Figure 2D show data from n=6 mice per genotype. Figure 3C-D show data from n=3 mice per genotype.

> *(4) The data on Fgf5 RNA expression presented in Figure 2E are not sufficiently convincing. The perimeter and cytoarchitecture of the cerebellum are difficult to see and the higher magnification shown in 2F should be indicated in 2E.*

The lack of foliation in Sufu-cKO cerebellum is clear particularly when visualizing the perimeter via DAPI labeling (Figure 2E). The expression area of FGF5 is also visibly larger, given that all images in Figure 2E are presented in the same scale (scale bars = 500 um).

> *(5) The data presented in Figure 3 are not sufficiently convincing. The number of cells double positive for pErk and KI67 (Figure 3B) are difficult to see and appear to be few, suggesting the quantification may be unreliable.*

We used KI67+ expression to provide a molecular marker of regions to be quantified in both WT and Sufu-cKO sections. Quantification of labeled cells were performed in images obtained by confocal microscopy, enabling imaging of 1-2 um optical slices since Ki67 or pERK expression might not localize within the same cellular compartments. We relied on continuous DAPI nuclear staining to distinguish individual cells in each optical slice and the colocalization of of Ki67 and pERK. All quantification were performed from 2-3 20 um cerebellar sections of 3-6 independent mice per genotype analyzed. Individual points in the bar graphs represent the average cell number (quantified from 2-3 sections) from each mice.

> *(6) The data presented in Figure 4F-J would be more convincing with quantification. The Sufu;p53-dKO appears to have a thickened EGL across the entire vermis perimeter, and very little foliation, relative to control and single cKO cerebella. This is a more widespread effect than the more localized foliation disruption in the Sufu-cKO.*

We agree with the reviewers that quantification of these phenotypes provide a solid measure of the defects. The phenotypes of Sufu:p53-dKO cerebellum are so profound requiring in-depth characterization that will be the focus of future studies.

> *(7) Figure 5 does not convincingly summarize the results. Blue and purple cells in sagittal cartoon are not defined. Which cells express Fgf5 (or other Fgfs) has not been determined. The yellow cells are not defined in relation to the initial cartoon on the left.*

The revised manuscript will address this confusion by clearly labeling the cells and their roles in the schematic diagram.

> ***Reviewer #2 (Public Review):***
>
> *Summary:*
>
> *Mutations in SUFU are implicated in SHH medulloblastoma (MB). SUFU modulates Shh signaling in a context-dependent manner, making its role in MB pathology complex and not fully understood. This study reports that elevated FGF5 levels are associated with a specific subtype of SHH MB, particularly in pediatric cases. The authors demonstrate that Sufu deletion in a mouse model leads to abnormal proliferation of granule cell precursors (GCPs) at the secondary fissure (region B), correlating with increased Fgf5 expression. Notably, pharmacological inhibition of FGFR restores normal cerebellar development in Sufu mutant mice.*
>
> *Strengths:*
>
> *The identification of increased FGF5 in subsets of MB is novel and a key strength of the paper.*
>
> *Weaknesses:*
>
> *The study appears incomplete despite the potential significance of these findings. The current paper does not fully establish the causal relationship between Fgf5 and*

abnormal cerebellar development, nor does it clarify its connection to SUFU-related MB. Some conclusions seem overstated, and the central question of whether FGFR inhibition can prevent tumor formation remains untested.

Reviewer #3 (Public Review):

Summary:

The interaction between FGF signaling and SHH-mediated GNP expansion in MB, particularly in the context of Sufu LoF, has just begun to be understood. The manuscript by Yabut et al. establishes a connection between ectopic FGF5 expression and GNP over-expansion in a late-stage embryonic Sufu LoF model. The data provided links region-specific interaction between aberrant FGF5 signaling with the SHH subtype of medulloblastoma. New data from Yabut et al. suggest that ectopic FGF5 expression correlates with GNP expansion near the secondary fissure in Sufu LoF cerebella. Furthermore, pharmacological blockade of FGF signaling inhibits GNP proliferation. Interestingly, the data indicate that the timing of conditional Sufu deletion (E13.5 using the hGFAP-Cre line) results in different outcomes compared to later deletion (using Math1-cre line, Jiwani et al., 2020). This study provides significant insights into the molecular mechanisms driving GNP expansion in SHH subgroup MB, particularly in the context of Sufu LoF. It highlights the potential of targeting FGF5 signaling as a therapeutic strategy. Additionally, the research offers a model for better understanding MB subtypes and developing targeted treatments.

Strengths:

One notable strength of this study is the extraction and analysis of ectopic FGF5 expression from a subset of MB patient tumor samples. This translational aspect of the study enhances its relevance to human disease. By correlating findings from mouse models with patient data, the authors strengthen the validity of their conclusions and highlight the potential clinical implications of targeting FGF5 in MB therapy.

The data convincingly show that FGFR signaling activation drives GNP proliferation in Sufu, conditional knockout models. This finding is supported by robust experimental evidence, including pharmacological blockade of FGF signaling, which effectively inhibits GNP proliferation. The clear demonstration of a functional link between FGFR signaling and GNP expansion underscores the potential of FGFR as a therapeutic target in SHH subgroup medulloblastoma.

Previous studies have demonstrated the inhibitory effect of FGF2 on tumor cell proliferation in certain MB types, such as the ptc mutant (Fogarty et al., 2006)(Yaguchi et al., 2009). Findings in this manuscript provide additional support suggesting multiple roles for FGF signaling in cerebellar patterning and development.

Weaknesses:

In the GEO dataset analysis, where FGF5 expression is extracted, the reporting of the P-value lacks detail on the statistical methods used, such as whether an ANOVA or t-test was employed. Providing comprehensive statistical methodologies is crucial for assessing the rigor and reproducibility of the results. The absence of this information raises concerns about the robustness of the statistical analysis.

The revised manuscript will include the following detailed explanation of the statistical analyses of the GEO dataset:

For the analysis of expression values of FGF5 (ENSG00000138675), we obtained these values using Geo2R (Barrett et al., 2013), which directly analyze published human MB subtype

expression arrays from accession no. GSE85217 (Cavalli et al., 2017). GEO2R is an interactive web tool that compares expression levels of genes of interest (GOI) between sample groups in the GEO series using original submitter-supplied processed data tables. We simply entered the GOI Ensembl ID and organized data sets according to age and MB subgroup or MBSHH subtype classifications. GEO2R results presented gene expression levels as a table ordered by FDR-adjusted (Benjamini & Hochberg) p-values, with significance level cut-off at 0.05, processed by GEO2R's built-in limma statistical test. Resulting data were subsequently exported into Prism (GraphPad). We generated scatter plots presenting FGF5 expression levels across all MB subgroups (Figure 1A) and MBSHH subtypes (Figure 1D). We performed additional statistical analyses to compare FGF5 expression levels between MB subgroups and MBSHH subtypes and graphed these data as violin plots (Figure 1B, 1C, and 1E). For these analyses, we used one-way ANOVA with Holm-Sidak's multiple comparisons test, single pooled variance. *P* value ≤0.05 was considered statistically significant. Graphs display the mean ± standard error of the mean (SEM). Sample sizes were:

Author response table 1.

MB^{WNT} n=70	$MB^{SHHα}$ n=66
MB^{SHH} n=224	$MB^{SHHβ}$ n=35
MB^{GR3} n=143	$MB^{SHHγ}$ n=47
MB^{GR4} n=326	$MB^{SHHδ}$ n=76

> *Another concern is related to the controls used in the study. Cre recombinase induces double-strand DNA breaks within the loxP sites, and the control mice did not carry the Cre transgene (as stated in the Method section), while Sufu-cKO mice did. This discrepancy necessitates an additional control group to evaluate the effects of Cre-induced double-strand breaks on phosphorylated H2AX-DSB signaling. Including this control would strengthen the validity of the findings by ensuring that observed effects are not artifacts of Cre recombinase activity.*

The breeding scheme we used to generate homozygous SUFU conditional mutants will not generate pups carrying only hGFAP-Cre. Thus, we are unable to compare expression of gH2AX expression in littermates that do not carry loxP sites. The reviewer is correct in pointing out the possibility of Cre recombinase activity inducing double-strand breaks on its own. However, it is likely that any hGFAP-Cre induced double-strand breaks does not sufficiently cause the phenotypes we observed in homozygous mutants (Sufu-cKO) mice because the cerebellum of mice carry heterozygous SUFU mutations (hGFAP-Cre;Sufu-fl/+) do not display the profound cerebellar phenotypes observed in Sufu-cKO mice. We cannot rule out, however, any undetectable abnormalities that could be present which may require further analyses.

> *Although the use of the hGFAP-Cre line allows genetic access to the late embryonic stage, this also targets multiple celltypes, including both GNPs and cerebellar glial cells. However, the authors focus primarily on GNPs without fully addressing the potential contributions of neuron-glial interaction. This oversight could limit the understanding of the broader cellular context in which FGF signaling influences tumor development.*

The reviewer is correct in that hGFAP-Cre also targets other cell types, such as cerebellar glial cells, which are generated when Cre-expression has begun. It is possible that cerebellar glial cell development is also compromised in Sufu-cKO mice and may disrupt neuron-glial interaction, due to or independently of FGF signaling. In-depth studies are required to interrogate how loss of SUFU specifically affect development of cerebellar glial cells and influence their cellular interactions in the developing cerebellum.

> ***Recommendations for the authors:***
>
> ***Editorial Comments:***
>
> *The reviewers suggest a number of steps to improve the manuscript that include additional experiments and a deeper analyses and re-evaluation of existing data. Short of significant new experiments, there appears to be number of straightforward analyses that can improve the study:*
>
> *(1) Reanalyses of statistical and quantitative approaches used (e.gs FDR correction, cerebellar deficits, GEO analyses.*

The revised manuscript will include detailed information on the statistical and quantitative approaches as addressed in our response to the reviewer's comments.

> *(2) More clear presentation of qualitative labeling approaches (immunohistochemistry and in situ hybridization).*

A detailed description of the protocols used will be included in the methods section for labeling methods in the revised manuscript.

> ***Reviewer #1 (Recommendations For The Authors):***
>
> *AZD4547 treatment of the dKO mice would provide more convincing evidence that FGF-targeted treatments could curtail tumor growth in these mice or refute the suggestion that FGF-targeted treatment could prevent tumor growth.*

We agree that performing AZD4547 treatment on Sufu-dKO mice will strengthen these studies. However, we are unable to address since these mice are now unavailable. We hope that future studies will address these.

> *Atoh1 is referred to as Math1 (older nomenclature) and should be corrected.*

The revised manuscript will include this change in nomenclature.

> *Check verb tense throughout the manuscript.*

We will edit the manuscript further to check verb tenses prior to submission of the revised manuscript.

> ***Reviewer #2 (Recommendations For The Authors):***
>
> *Specific Comments:*
>
> *(1) The identification of increased FGF5 in subsets of MB is novel and a key strength of the paper. However, the causal relationship between FGF5 and MB remains unestablished. Based on the current data, FGF5 can only be considered a biomarker for stratifying MB.*

We agree with the reviewer that our studies do not provide direct evidence that FGF5 cause MB. Future investigation focusing on determining if FGF5 inhibition leads to phenotypic rescue will strongly establish the relationship between FGF5 and MB. The reviewer is also correct that our studies reveal that FGF5 acts as a potential biomarker, as we mentioned in the Discussion section.

> *(2) The upregulation of Fgf5 in Sufu-deficient cerebella is crucial to this study, yet the presented data are unconvincing to support this conclusion. In comparing Fgf5 expression between WT and Sufu mutants (Figures 2E, F and 4I), the cerebellar sections differ significantly, with mutant sections seemingly from a more lateral position. The authors should provide images of mutant sections from more comparable positions to accurately assess the effect of Sufu deficiency on Fgf5 expression. Additionally, the signals in Figure 2F resemble non-specific backgrounds rather than specific RNAscope signals.*

The WT and mutant sections analyzed were carefully selected from comparable levels. The abnormal foliation in Sufu-cKO make the mutant sections look like they are from the lateral cerebellum.

Figure 2F (enlarged regions) point to punctate RNAScope signals which is characteristic of this labeling method (see RBFOX3 or GFAP labeling in DAPI-labeled cells in the mouse brain at https://acdbio.com/science/applications/research-areas/neuroscience). The higher number of punctate signals in some, but not all, DAPI-labeled cells in Figure 2F indicate that the FGF5 RNAScope signal is specific.

> *(3) Jiwani et al. (2020) reported that Fgf8 also expressed in region B of the EGL, is upregulated in Sufu-deficient cerebella and is necessary and sufficient for Sufu mutant GCP proliferation. The current study does not distinguish whether the FGFR inhibitor AZD4547 blocks Fgf5 and Fgf8 function in restoring cerebellar histology in Sufu mutants.*

AZD4547 potently inhibits FGFR1, FGFR2, and FGFR3 autophosphorylation (Gavine et al., Cancer Research, 2012). FGF8 is reported to bind to these receptors (Ornitz and Itoh, 2015). Thus, the reviewer is correct that the studies will not distinguish between FGF5 or FGF8 activity. Further investigation on FGF8 expression and the effects of its inhibition in the Sufu-cKO neonatal cerebellum will determine whether tumorigenic processes are driven by either FGF5 or FGF8. Nevertheless, we postulate that FGF5 is exerting a greater effect in activating FGF signaling in the developing cerebellum given that it is highly expressed along the external granule layers of the developing cerebellum (Author response image 3).

Author response image 3.

Expression of FGF5 and FGF8 in the P4 mouse cerebellum (Allen Brain Atlas, https://developingmouse.brain-map.org)

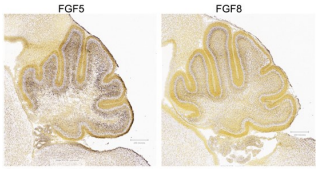

> *(4) The authors should show whether AZD4547 treatment restores normal Fgf5 expression. Importantly, they need to test whether AZD4547 rescues the proliferation defect observed in Sufu;p53 double mutants.*

We agree that performing AZD4547 treatment on Sufu-dKO mice will strengthen these studies. However, we are unable to address since these mice are now unavailable. We hope that future studies will address these.

> *(5) Jiwani et al. (2020) showed that deleting Sufu with Atoh1-Cre promotes Gli3R and suppresses Gli2 levels, leading to increased cell proliferation and delayed cell cycle exit in the central lobe. The findings of the current study (Supplementary Figure 1) seem to differ from this previous report, yet both studies conclude that Sufu-KO disrupts differentiation. The authors should provide an explanation for this discrepancy.*

Our results align completely with the findings by Jiwani et al. (2020). Both studies showed reduced levels of Gli3R, showing nearly 50% reduction, when Sufu is deleted (see Figure 4A-4D in Jiwani et al., 2020).

> *(6) The hGFAP-Cre mouse line is used to delete Sufu from the cerebellum, but it is not commonly used for GCP-specific deletion. The authors need to provide a reference or more details on the temporal and spatial activity of the Cre line, as the cited paper describes its generation but offers little information on its activity in the developing cerebellum.*

We appreciate the reviewer's reminder to include the reference for the Schuller et al. 2008 paper. This study characterized the hGFAP-Cre temporal and spatial expression in the developing cerebellum, including granule cell precursors. We will include this reference in the revised manuscript.

> *(7) Based on the provided data, it is difficult to determine which cell types express Fgf5. Given that hGFAP-cre may delete Sufu in other cerebellar cell types, the authors should demonstrate that Fgf5 is expressed in granule cells or granule cell precursors.*

Future studies will focus on further characterization of the role of FGF5 in cerebellar development, including the identity cells expressing FGF5. The reviewer is correct in that hGFAP-Cre also targets other cell types and that Sufu deletion in these cells induced ectopic FGF5 expression.

> *(8) The provided data show an increase in pERK+ cells in GCPs at the secondary fissure. This increase may simply reflect an accumulation of GCPs. It is unconvincing that there is an increase in pERK due to the loss of Sufu.*

The reviewer is correct that the increase in GCPs will also result increase the number of pERK+ cells. To control for this, our quantification reflects the number of cells per unit area where Ki67+ cells. With these parameters, we found that there is an increased density of pERK+ cells in a given Ki67+ region. All quantification were performed from 2-3 20 um cerebellar sections of 3-6 independent mice per genotype analyzed. Individual points in the bar graphs represent the average cell number (quantified from 2-3 sections) from each mice.

> *(9) No data are provided on MB formation in Sufu-cKO; p53- mutants, and it is unknown whether FGFR inhibitors block tumor formation.*

We agree that performing AZD4547 treatment on Sufu-dKO mice will strengthen these studies. However, we are unable to address since these mice are now unavailable. We hope that future studies will address these.

> *(10) The authors frequently mention "preneoplastic lesions" of GCPs in Sufu mutant mice. What evidence supports this claim?*

Preneoplastic lesions are defined as cells carrying genetic and phenotypic alterations that show higher risk of malignancy (such as MB) but lack the capacity to grow autonomously in

the absence of a secondary factor (Feo et al., 2011). In Sufu-cKO mice, we see abnormally proliferating and behaving granule precursor cells that do not grow autonomously, in the absence of a p53 LOF. The combined deletion of Sufu and p53 transforms these cells to become neoplastic.

> *(11) Fgf5 is normally expressed in region B. What is its potential function? Does AZD4547 affect normal development?*

Future studies will focus on further characterization of the role of FGF5 in cerebellar development, including the identity cells expressing FGF5. Regarding AZD4547, we did not observe any obvious difference between AZD4547-treated and vehicle-treated cerebelli. These indicate that AZD4547 inhibition of FGFRs under physiologic conditions does not significantly disrupt normal cerebellar development.

> *(12) Figure 3G: It is unclear which specimens were treated with AZD4547. The authors mention treatment in line 281 but contradict themselves in the figure legend.*

We thank the reviewer for pointing out this typo. Cerebellar tissues shown in Figure 3G were all treated with AZD4547. The figure legend will be corrected in the revised manuscript.

> *(13) Figure 4J: The higher magnification images of the pERK/Ki67 staining appear identical in the control and Sufu;p53-dKO. The authors need to correct the mistake.*

We thank the reviewer for pointing this out. We will correct this figure in the revised manuscript.

> *Minor Comments:*
>
> *(1) Whenever possible, images comparing WT and mutants should be presented at the same scale within a figure. For example, readers might easily conclude that mutant brains are smaller than controls in Figure 4G.*

Unfortunately, because the cerebellum of Sufu;p53-dKO mice are significantly bigger, we are unable to show the whole cerebellum in the same scale in Figure 4G. We wanted to emphasize the significant and abnormal cerebellar growth in this figure.

> *(2) The figure legend for Supplementary Figure 2 is missing.*

Thank you for pointing this out. We will add a figure legend in this Supplementary data in the revised manuscript.

> *(3) The authors state that the expansion of Pax6+ GNPs in the newborn Sufu-cKO cerebellum (Figure 2) occurs in similar anatomical subregions where infantile MB tumors typically arise (Tan et al., 2018). The cited paper describes more abundant SHH MB in the cerebellar hemisphere. The authors need to elaborate on their statement to clarify this point.*

The reviewer is correct in that Tan et al., 2018 observed tumors arising from the cerebellar hemisphere. More specifically, these tumors arise in the posterior/ventral regions of the cerebellar hemispheres (Figure 2 in Tan et al., 2018). Similarly, Sufu-cKO mice have more severe defects in the posterior/ventral regions of the cerebellar hemisphere (Figures 2A and 3F) and therefore corroborate the findings by Tan et al., that abnormal SHH signaling in these regions results in increased sensitivity to MB formation.

> ***Reviewer #3 (Recommendations For The Authors):***
>
> *Figure1 [Upregulated FGF5 expression in MBS-HH tumors]*
>
> *- Statistical analysis from the Geo expression dataset does not provide enough detail. At least, the authors should mention whether they have made any adjustments from the default settings and how they extracted/plotted the FGF5 expression (Figure 1BCE).*

For the analysis of expression values of FGF5 (ENSG00000138675), we obtained these values using Geo2R (Barrett et al., 2013), which directly analyze published human MB subtype expression arrays from accession no. GSE85217 (Cavalli et al., 2017). GEO2R is an interactive web tool that compares expression levels of genes of interest (GOI) between sample groups in the GEO series using original submitter-supplied processed data tables. We simply entered the GOI Ensembl ID and organized data sets according to age and MB subgroup or MBSHH subtype classifications. GEO2R results presented gene expression levels as a table ordered by FDR-adjusted (Benjamini & Hochberg) p-values, with significance level cut-off at 0.05, processed by GEO2R's built-in limma statistical test. Resulting data were subsequently exported into Prism (GraphPad). We generated scatter plots presenting FGF5 expression levels across all MB subgroups (Figure 1A) and MB^{SHH} subtypes (Figure 1D). We performed additional statistical analyses to compare FGF5 expression levels between MB subgroups and MB^{SHH} subtypes and graphed these data as violin plots (Figure 1B, 1C, and 1E). For these analyses, we used one-way ANOVA with Holm-Sidak's multiple comparisons test, single pooled variance. *P* value ≤0.05 was considered statistically significant. Graphs display the mean ± standard error of the mean (SEM). See Author response table 1 for sample sizes.

> *Figure 3 [Ectopic activation of FGF signaling in the EGL of P0 Sufu-cKO cerebellum]*
>
> *- Gil1-lz mice reference wrong. Correct Bai CB, et al. 2002*
>
> *- Generation of Sufu-cKO;Gli1-LacZ triple transgenic mice not described*
>
> *- Veh vs. treated not labelled (Figure 3F)*

We will address these minor text changes in the revised manuscript. A more detailed description of the generation of Sufu-cKO;Gli1-LacZ triple transgenic will also be included in the Methods section.

> *Figure 5 [Proposed model]*
>
> *- In the text, Figure 5 is mistaken for Figure 8.*

We will address these minor text changes in the revised manuscript.

https://doi.org/10.7554/eLife.100767.2.sa0